FRAMEWORK AND METHODOLOGY FOR RISK-BASED BRIDGE AND TUNNEL ASSET MANAGEMENT

Objective Risk Assessment and Network Level Evaluation

TECHNICAL REPORT DOCUMENTATION PAGE

1. Report No. https://archives.pdx.edu/ds/psu/42287	2. Government Accession No.	3. Recipient's Catalog No.
4. Title and Subtitle Framework and Methodology for Risk-Based Bridge and Tunnel Asset Management: Objective Risk Assessment and Network Level Evaluation		5. Report Date August 2, 2024 6. Performing Organization Code:
7. Author(s) David Y. Yang (ORCID: 0000-0003-0959-6333) Arash Khosravifar (ORCID: 0000-0002-7137-6289) Diane Moug (ORCID: 0000-0001-5256-0438) Portland State University Avinash Unnikrishnan (ORCID: 0000-0001-6737-0485) University of Alabama at Birmingham		8. Performing Organization Report No.
9. Performing Organization Name and Address Portland State University Department of Civil and Environmental Engineering 1920 SW 4th Avenue, Office 301F Portland, OR 97201 DUNS: 052226800		10. Work Unit No. 11. Contract or Grant No. 693JJ321C000030
12. Sponsoring Agency Name and Address Office of Bridges and Structures Federal Highway Administration 1200 New Jersey Ave SE Washington, DC 20590		13. Type of Report and Period 14. Sponsoring Agency Code
15. Supplementary Notes		

16. Abstract

This report presents the results of the project on establishing a general framework and methodology for risk-based bridge and tunnel asset management. The research was carried out at Portland State University in collaboration with engineers and officials at Oregon Department of Transportation (ODOT) and Federal Highway Administration (FHWA). The primary goal of the research is to achieve risk-based transportation asset management based on (a) objective and consistent risk assessment and (b) effective prioritization and optimization of intervention strategies. This report presents methods and findings in the base phase (Phase I) of the project, which is focused on the objective and consistent risk assessment suitable for network-level transportation asset management. Specifically, the following three tasks were conducted: (a) establish general methodology for objective risk assessment of deteriorating assets; (b) achieve objective agency risk assessment in transportation asset management systems; (c) develop effective and efficient approaches to network-level user risk assessment.

17. Key Words Objective asset risk assessment Performance risk of transportation networks Performance-based asset management	18. Distribution Statement No restrictions. This document is available to the public through the National Technical Information Service, Springfield, VA 22161. http://www.ntis.gov

19. Security Classif. (of this report) Unclassified	20. Security Classif. (of this page) Unclassified	21. No. of Pages	22. Price

Form DOT F 1700.7 (8-72) Reproduction of completed page authorized.

SI* (MODERN METRIC) CONVERSION FACTORS

APPROXIMATE CONVERSIONS TO SI UNITS

Symbol	When You Know	Multiply By	To Find	Symbol
		LENGTH		
in	inches	25.4	millimeters	mm
ft	feet	0.305	meters	m
yd	yards	0.914	meters	m
mi	miles	1.61	kilometers	km
		AREA		
in^2	square inches	645.2	square millimeters	mm^2
ft^2	square feet	0.093	square meters	m^2
yd^2	square yard	0.836	square meters	m^2
ac	acres	0.405	hectares	ha
mi^2	square miles	2.59	square kilometers	km^2
		VOLUME		
fl oz	fluid ounces	29.57	milliliters	mL
gal	gallons	3.785	liters	L
ft^3	cubic feet	0.028	cubic meters	m^3
yd^3	cubic yards	0.765	cubic meters	m^3
	NOTE: volumes greater than 1000 L shall be shown in m^3			
		MASS		
oz	ounces	28.35	grams	g
lb	pounds	0.454	kilograms	kg
T	short tons (2000 lb)	0.907	megagrams (or "metric ton")	Mg (or "t")
		TEMPERATURE (exact degrees)		
°F	Fahrenheit	5 (F-32)/9 or (F-32)/1.8	Celsius	°C
		ILLUMINATION		
fc	foot-candles	10.76	lux	lx
fl	foot-Lamberts	3.426	candela/m^2	cd/m^2
		FORCE and PRESSURE or STRESS		
lbf	poundforce	4.45	newtons	N
lbf/in^2	poundforce per square inch	6.89	kilopascals	kPa

APPROXIMATE CONVERSIONS FROM SI UNITS

Symbol	When You Know	Multiply By	To Find	Symbol
		LENGTH		
mm	millimeters	0.039	inches	in
m	meters	3.28	feet	ft
m	meters	1.09	yards	yd
km	kilometers	0.621	miles	mi
		AREA		
mm^2	square millimeters	0.0016	square inches	in^2
m^2	square meters	10.764	square feet	ft^2
m^2	square meters	1.195	square yards	yd^2
ha	hectares	2.47	acres	ac
km^2	square kilometers	0.386	square miles	mi^2
		VOLUME		
mL	milliliters	0.034	fluid ounces	fl oz
L	liters	0.264	gallons	gal
m^3	cubic meters	35.314	cubic feet	ft^3
m^3	cubic meters	1.307	cubic yards	yd^3
		MASS		
g	grams	0.035	ounces	oz
kg	kilograms	2.202	pounds	lb
Mg (or "t")	megagrams (or "metric ton")	1.103	short tons (2000 lb)	T
		TEMPERATURE (exact degrees)		
°C	Celsius	1.8C+32	Fahrenheit	°F
		ILLUMINATION		
lx	lux	0.0929	foot-candles	fc
cd/m^2	candela/m^2	0.2919	foot-Lamberts	fl
		FORCE and PRESSURE or STRESS		
N	newtons	0.225	poundforce	lbf
kPa	kilopascals	0.145	poundforce per square inch	lbf/in^2

TABLE OF CONTENTS

LIST OF FIGURES

LIST OF TABLES

LIST OF ABBREVIATIONS AND SYMBOLS

API	application programming interface
BMS	bridge management system
CDF	cumulative distribution function
CR	condition rating
CSV	comma-separated values
DS	damage state
FHWA	Federal Highway Administration
FEMA	Federal Emergency Management Agency
IM	intensity measure
MC	Monte Carlo
MCMC	Markov chain Monte Carlo
NBI	National Bridge Inventory
NIST	National Institute of Standards and Technology
OD	origin-destination
ODOT	Oregon Department of Transportation
PDF	probability density function
PGA	peak ground acceleration
SA	spectral acceleration
TMCMC	transitional Markov chain Monte Carlo
TAM	transportation asset management
USGS	United States Geological Survey
a	annual deterioration rate
cq_f	"failure" or service disruption consequence
$cq(ds)$	consequence associated with a DS
$C_{NET,0}$	system-level consequences without any damage
$C_{NET}(\mathbf{s})$ or $C(\mathbf{s})$	system-level consequences given a system state $\mathbf{s}$

$\overline{CQ}(im_{ev})$	expected consequence under a hazard scenario with an intensity level equal to im_{ev}
CR	random variable representing CR
d	distance between a site and a fault in kilometers
$DS\|IM$	random variable representing DS conditioned on IM
f_i	capacity of link i
IM	random variable representing IM of an adverse event
im_i	IM in the ith hazard scenario
M	magnitude of an earthquake
n_{lane}	number of lanes
$p_{DS\|IM}$	probability of a specific DS conditioned on a specific IM level
$p_f(cr)$	"failure" or service disruption probability conditioned on a CR
$p(\mathbf{s})$	probability of a system state $\mathbf{s}$
$PGA_m^{(ds)}(0)$	median PGAs, associated with damage state ds, at the start of the service life (pristine state)
$PGA_m^{(ds)}(t)$	median PGAs, associated with damage state ds, after t years in service
$p_{IM}(im_{ev})$	likelihood of a hazard scenario with an intensity level equal to im_{ev}
$p_{f,i}$ and C_i	failure probability and asset-level consequence associated with asset i
r	real annual discount rate
$R_{det}(t)$	deterioration risk in year t
$R_{L,total}(mx)$	total lifetime risk with maintenance
$R_{L,total}(na)$	total lifetime risk without maintenance
$R_{xev}(t)$	extreme event risk in year t
$\boldsymbol{T}(\boldsymbol{\theta})$	transformation function of $\boldsymbol{\theta}$ converted to system state
v_{lane}	speed limit on a traffic lane
v_{nom}	nominal speed on a traffic lane
w_i	responsibility weight of the ith hazard scenario

β	reliability index
η_i	integration weights of a Gaussian quadrature
λ_{IM}	annual rate of exceedance for IM
ξ_i	integration points of a Gaussian quadrature
σ	dispersion factor of the PGA
Φ	CDF of a standard normal distribution
θ and $\boldsymbol{\theta}$	one and one set of hidden variables, respectively, for system state

FRAMEWORK AND METHODOLOGY FOR RISK-BASED BRIDGE AND TUNNEL ASSET MANAGEMENT: OBJECTIVE RISK ASSESSMENT AND NETWORK LEVEL EVALUATION

EXECUTIVE SUMMARY

INTRODUCTION

This report presents the results of the project on establishing a general framework and methodology for risk-based bridge and tunnel asset management. The research was carried out at Portland State University in collaboration with engineers and officials at Oregon Department of Transportation (ODOT) and Federal Highway Administration (FHWA). The primary goal of the research is to achieve risk-based transportation asset management based on (a) objective and consistent risk assessment and (b) effective prioritization and optimization of intervention strategies. This report presents methods and findings in the base phase (Phase I) of the project, which is focused on the objective and consistent risk assessment suitable for network-level transportation asset management. Specifically, the following three tasks were conducted to fulfill the general goal of Phase I:

- Establish methodology for objective risk assessment due to deterioration and extreme events;
- Achieve objective agency risk assessment in transportation asset management systems;
- Develop effective and efficient approaches to network-level user risk assessment.

BACKGROUND

Management of critical transportation assets such as bridges and tunnels has traditionally focused on condition preservation through carefully planned life-cycle activities within a budgetary limit. Such plans are enacted to impede deterioration and/or accommodate increasing demand. Although there are calls to consider various risks from extreme events, existing approaches to risk assessment in transportation asset management rely heavily on engineering judgement, past experience, and limited data indicators that roughly correlate with hazard intensities, bridge vulnerabilities, and damage consequences. Existing approaches score and weight hazard types and vulnerabilities that compete against other bridge needs. This subjective or empirical approach to risk assessment contrasts to more objective methods that are underpinned by quantitative models of hazards, vulnerabilities, and consequences. Nonetheless, these quantitative models do not fully consider the effects of deterioration on structural vulnerability under extreme events, thus hindering their direct application in transportation asset management.

The gap between transportation asset management and objective risk assessment leads to (a) inconsistency between risks assessed by different agencies or different experts and (b) neglect or inaccurate estimates of risks compounded by asset deterioration. As a result, resources may be allocated inefficiently due to (a) unreliable estimates of project benefits and (b) lack of coordination between condition preservation and risk mitigation needs. This project aims to resolve this issue by presenting a unified framework for risk-based transportation asset management, focusing on critical transportation structures such as bridges and tunnels.

Phase I of the project was started with the establishment of a general methodology to unify the assessments of structural deterioration and risks under extreme events. Direct economic risk to an agency and indirect societal risk to road users were then considered respectively. For agency risk assessment, the focus was on the viability and implications of objective risk assessment in transportation management (in particular, bridge management systems). For user risk assessment, the pivot was to develop new methods to overcome computational challenges during risk assessment related to system performance after hazard events and subsequent bridge damage. These challenges arise because the roles of different assets to system performance are interdependent among networked assets. Findings from the research work are presented below.

FINDINGS

Risk due to Deterioration and Extreme Events

To unify deterioration and risk assessments, deterioration-induced service disruption can be treated as a hazard and integrated with risk assessment under extreme events. In this manner, total lifetime risk from deterioration and extreme events is determined to facilitate risk-based transportation asset management. The formulated assessment methodology is underpinned by objective risk assessment consistent with other frameworks for modeling infrastructure risk and resilience. Integrated risk assessment, as described in this project, is also able to consider exacerbated extreme event risk due to structural deterioration.

Input needs for this new methodology are clarified. Specifically, to estimate deterioration risk, the input data and models include (a) deterioration models with respect to asset condition states or ratings, (b) probabilities of service disruption corresponding to different condition ratings, and (c) cost estimates for deterioration-induced service disruption. For extreme event risk, objective risk assessment relies on (a) hazard characterization curves (i.e., rate vs. intensity), (b) fragility functions of different structural archetypes for various damage states, and (c) cost estimates associated with different damage states. Potential sources and methods to obtain these inputs are detailed in the report. Data and knowledge gaps are identified, including standardized procedures to derive service disruption probabilities, lack of widely accepted fragility curves of deteriorated assets, reliable cost estimates for deterioration-induced service disruption, and sufficient data for non-seismic extreme events.

Objective Risk Assessment within Transportation Asset Management Systems

Rather than rely on experts to elicit hazard scenarios considered in risk assessment, a new approach is developed to automatically generate these hazard scenarios weighted by their importance to objective risk assessment. These weighted scenarios can be directly used in existing bridge and tunnel management systems. As the new approach is based on the rigorous formulation of risk integrals, the risk can be accurately and consistently estimated based on hazard characteristics, structural fragility, and damage consequences. Given the same number of hazard scenarios, Figure 1(a) shows the comparison between the risks estimated with the new method and with an existing analytical method within the reasonable capability of modern BMSs (termed the BMS approach).

Measured against the benchmark value obtained from a full probabilistic seismic risk analysis[1], the approach described in this document shows greater accuracy than the existing approach.

Additionally, the new approach can handle the interaction between structural deterioration and structural fragility under extreme events. As a result, it can be used to better quantify the benefit of life-cycle plans in terms of risk reduction under extreme events. The study compared two hypothetical life-cycle plans (i.e., maintenance sequences to restore pristine conditions) to demonstrate the implications of accurate risk assessment on asset management. Figure 1(b) presents the benefit-to-cost ratios of both plans, evaluated based on the new and the existing risk assessment approaches respectively. The comparison indicates that existing approach may not deliver reliable rankings of different life-cycle plans.

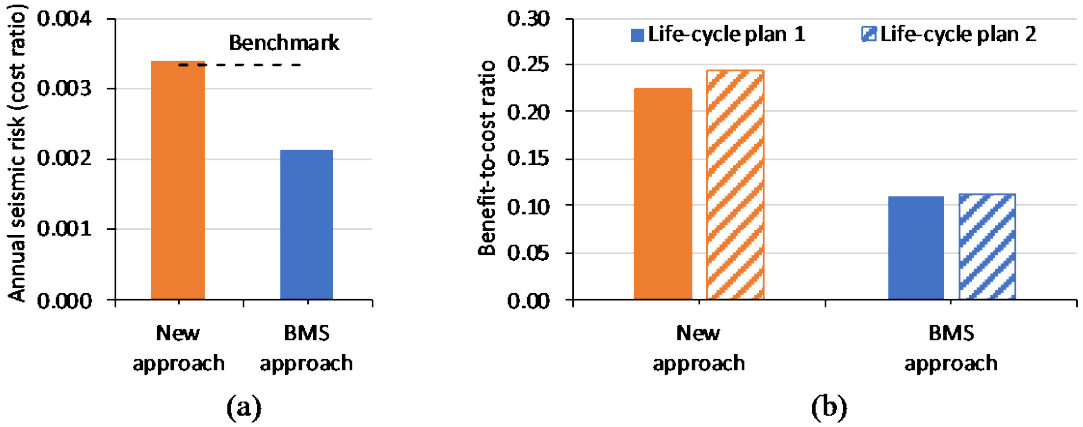

Figure 1 Benefit of objective risk assessment: (a) more accurate risk assessment and (b) more reliable comparison between life-cycle plans.

Mobility Risk Assessment for Large-Scale Transportation Networks

Indirect consequences to road users may exhibit the so-called network effect when the failure consequences of multiple assets greatly exceed the sum of failure consequences of individual assets. Examples include connectivity to public services, freight capacity within or throughput across a region, and extra travel cost due to congestion and detour. The need to simultaneously consider all asset conditions creates a significant computational challenge. In this project, an effective and efficient method is developed for indirect risk assessment involving network effects.

Compared to existing methods, the advantage of the new method lies in its abilities to handle large-scale systems with hundreds to thousands of assets and to robustly estimate risk dominated by a small number of low-probability, high-consequence events involving network effects. The effectiveness of the new method is demonstrated through a number of analytical examples and a real-world case study on the Oregon highway network. Based on the results from the analytical

[1] A full probabilistic seismic risk analysis refers herein to the evaluation of risk integral considering all possible intensity measure levels (return periods) of an extreme event and likely damage states of an asset due to the event.

examples, Figure 2(a) shows the accuracy of the new method in comparison to the benchmark and the results obtained from several existing methods.

In addition to assessing risk, the new method is also capable of identifying routes and assets that contribute the most to the network risk, thereby offering insights to intervention prioritization. Based on the case study results, Figure 2(b) presents the identified routes with bridges that significantly impact the network risk in terms of traffic throughput across the State of Oregon. Note that the results in Figure 2(b) hinges on several assumptions, e.g., the probabilities of service disruption for different bridges. Therefore, the results herein are for illustration purposes only and should not be considered as the exact vulnerable assets within the Oregon highway network.

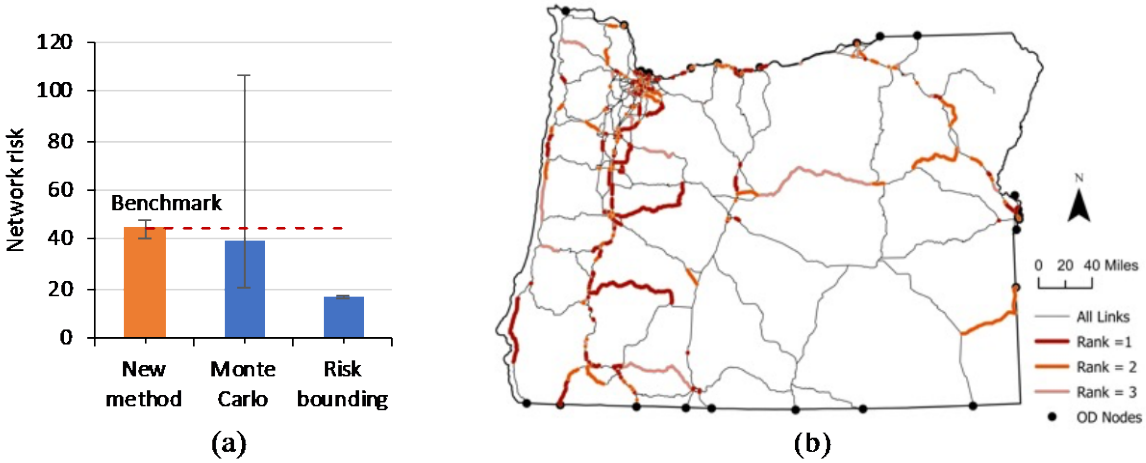

Figure 2 New method for indirect risk assessment: (a) effectiveness in assessing risk dominated by low probability, high consequence events (results from analytical examples) and (b) identified high-risk routes in Oregon highway network[1] (results from case study).

NEXT STEPS

Continuing with the Phase I study, Phase II of this project should focus on the validation of case study results related to network risk assessment. The validation process will examine and improve the various assumptions adopted in Phase I illustration. The identified links crucial to the system performance will be compared with the critical links established empirically by the Oregon Department of Transportation. Overlapping and differences should be investigated.

For future studies built upon this project, considerable efforts should be put into (a) the calibration of service disruption probabilities associated with deteriorated assets and (b) the establishment of time- or condition-based fragility curves that consider the effect of deterioration on structural vulnerability under extreme events.

[1] The results presented herein are limited by several assumptions, including assumed disruption probabilities for different links with bridges. The results are presented herein to illustrate the new method and should not be regarded as the true risk related to the Oregon highway network.

The project primarily uses earthquake hazards as an example of applying the framework and methodology, partly due to the relatively mature hazard, vulnerability, consequence models compared to non-seismic events. Nonetheless, the same approaches should be applicable to other hazards relevant to transportation systems such as floods and hurricanes. It is also worthwhile to explore other transportation performance indicators such as accessibility to critical services after disasters.

CHAPTER 1

INTEGRATING OBJECTIVE RISK ASSESSMENT AND TRANSPORTATION ASSET MANAGEMENT

1.1 INTRODUCTION

Bridge and tunnel asset management has traditionally focused on the condition preservation of a large stock of structures through carefully planned life-cycle activities within a budgetary limit (including inspections, maintenance, rehabilitation, and replacement). Such plans are enacted to impede deterioration and/or accommodate increasing demand. Although there are calls to consider risks from extreme events during life-cycle planning, existing approaches to risk assessment in transportation asset management (TAM) relied heavily on engineering judgement and past experience within a transportation agency (Western et al. 2016). The results from these approaches may, thus, vary due to personnel turnover and institutional changes.

The subjective approaches to risk assessment in TAM contrast to more objective approaches commonly used in several frameworks for risk assessment and resilience quantification, e.g., HAZUS developed by FEMA (2023) and IN-CORE developed by NIST (2023), among others. In these frameworks focusing on extreme events, risks are derived from physics-based and/or empirical quantitative models of hazards, vulnerabilities, and consequences, thereby allowing objective risk assessment with a minimum amount of subjectivity. Nonetheless, these risk assessment frameworks do not fully consider the deteriorated conditions of transportation assets[1], even if deterioration may affect the structural vulnerability (i.e., fragilities) under extreme events. For instance, HAZUS models do not consider the deterioration of bridge substructure, though the cracking and spalling of concrete cover due to rebar corrosion can significantly alter the seismic fragility curves (Bhandari 2023).

The gap between transportation asset management and hazard risk assessment leads to (a) inconsistency between risks assessed in TAM and common risk assessment frameworks and (b) neglect of extreme event risk compounded by asset deterioration. As a result, resources for transportation infrastructure may be allocated inefficiently due to the lack of coordination between condition preservation and risk mitigation needs. This project aims to resolve this issue by developing a unified framework for risk-based transportation asset management, focusing on critical transportation structures such as bridges and tunnels. To achieve this, Chapter 1 first introduces:

- a new perspective to consider asset deterioration using the concept of deterioration risk;
- a novel approach to integrating asset management goals and risk minimization principles.

[1] These methods do sometimes consider the implications of structural age on fragilities. This is mainly implemented to reflect the predominant design guidelines, which affect structural vulnerability under hazards. However, all assets are treated as if they are newly constructed based on the then predominant design guidelines and do not experience any deterioration in their service life.

1.2 OBJECTIVE RISK ASSESSMENT FROM ADVERSE EVENTS

The framework is built upon the objective risk assessment approaches in previously mentioned hazard analysis frameworks. In these frameworks, risk associated with an adverse event, commonly referred to as a risk integral, is expressed as follows (Basöz & Mander 1999; McGuire 2004; Baker et al. 2021):

$$R = \int_{im} \left[\sum_{ds} cq(ds) \cdot p_{DS|IM}(ds|im) \right] |\lambda'_{IM}(im)| dim$$

Equation 1.1 Risk integral (discrete damage states and average consequence)

where a lower-case variable (im and ds) = sample from a random variable (represented by its upper-case counterparts, IM and DS); IM = intensity measure (IM) of an adverse event; $\lambda_{IM}(im)$ = annual rate of exceeding im (a specific value for the intensity measure, referred hereafter as an intensity level), and $|\lambda'_{IM}(im)|$ becomes the absolute value of the gradient of $\lambda_{IM}(im)$; $DS|IM$ = damage states (DSs) conditioned on the intensity measure; $p_{DS|IM}(ds|im)$ = probability of a specific DS ds conditioned on a specific intensity level im; $cq(ds)$ = average consequence associated with a DS.

Equation 1.1 fully captures the probabilistic nature of a hazard, as reflected by the integration carried out over the PDF of the hazard intensity measure. This allows for the proper consideration of all hazard intensities relevant to a site of interest. This improvement contrasts to the existing methods within TAM where a small number of intensity levels, usually adopted based on intensities for design, are considered. Equation 1.1 also incorporates the uncertainty related to the structural vulnerability, as represented by the conditional probabilities associated with different DSs. These conditional probabilities can be obtained using fragility curves, which provide the probabilities of reaching or surpassing a specific damage state given an intensity level[1] (Buckle et al. 2006; Muntasir Billah & Shahria Alam 2015). Through Equation 1.1, risk can be objectively assessed with a hazard characterization model λ_{IM}, fragility curves to derive $p_{DS|IM}$, and the expected cost data for each DS $cq(ds)$. Risk can be objectively quantified without relying on expert elicitation with these models (e.g., using those provided in HAZUS).

The risk integral in Equation 1.1 has been used to assess risks from (a) a single source of hazards (e.g., earthquakes) or (b) hazards with independent (or weakly correlated) physical mechanisms (e.g., earthquakes and floods). In the latter case, the risk associated with each hazard can be considered separately, and the total risk due to multiple independent hazards is the summation of the risk values from different hazards. The assumption of independent hazards has been adopted in existing multi-hazard risk assessment approaches in TAM (Western et al. 2016). However, it should be noted that this assumption of independent hazards may fail to capture multi-hazard effects, e.g., when the genesis of hazards or the vulnerability of structures are correlated or interdependent. For instance, the deterioration of bridge substructure may increase structural

[1] The probabilities of reaching a damage state can then be calculated by subtracting the fragility value of the next worse damage state from the fragility value of the damage state under consideration.

vulnerability under seismic events. It is important to capture this interaction for the integration of asset management and risk assessment.

1.3 LIFETIME RISK DUE TO DETERIORATION

Deterioration risk of a structure can be attributed to the reduced load-carrying capacity due to environmental and mechanical stressors (e.g., corrosion and fatigue). Excessive deterioration may ultimately lead to structural closure or even unexpected failure. Poor condition is the single most significant contributor to bridge decommission in the US, accounting for 41.4% of all cases (Bektas & Albughdadi 2020). Deterioration-related bridge failure (including partial to total collapse) amounts to 6% to 9% of all bridge failure cases from 1987 to 2011 (Wardhana & Hadipriono, 2003; Cook, et al., 2015). Therefore, although asset management deals primarily with condition preservation, the goal of asset management can also be reinterpreted as risk reduction against deterioration. In this context, deterioration-related service disruption (or structural failure) can be treated as a particular hazard, allowing for a straightforward integration of condition preservation and risk mitigation.

In the context of Equation 1.1, the IM and DS associated with this deterioration hazard are described as follows. In bridge management systems (or TAM in general), the intensity of deterioration is usually measured by condition states or condition ratings such as in the National Bridge Inventory (NBI). Herein, the NBI condition ratings are used as intensity measure to quantify deterioration risk. In general, the lower the NBI rating is, the more likely the asset is to experience service disruption (or even unexpected failure). Note that other descriptors of deterioration, such as health index (Inkoom et al. 2017), can also be used in this context as the intensity measure of deterioration risk. "Survival" and "failure" under normal traffic conditions are considered as two DSs conditioned on different condition ratings. Note that "failure" herein refers to any types of severe service disruption that can include planned decommission such as bridge closure before the end of service life. Deterioration risk R_{det} can be derived from Equation 1.1 as follows:

$$\begin{aligned} R_{det} &= \int_{im} \left[\sum_{ds} cq(ds) p_{DS|IM}(ds|im) \right] |\lambda'_{IM}(im)| dim \\ &= \sum_{cr} cq_f \cdot p_f(cr) \cdot p_{CR}(cr) \end{aligned}$$

Equation 1.2 Deterioration risk derived from the risk integral

where cq_f = failure consequence (note that only failure DS incurs cost); CR = condition rating used to reflect intensity of deterioration; $p_f(cr)$ = annual failure rate conditioned on different CR used to model structural vulnerability to deterioration. As the condition ratings are discrete values, the integral over IM in Equation 1.1 becomes a summation across different condition ratings in Equation 1.2.

For a specific year of interest, Equation 1.2 estimates the annual deterioration risk corresponding to the probability distribution of projected CRs in that year. Unlike stationary extreme events such

as earthquakes, the CR probabilities vary over time due to deterioration. This deterioration process (manifested by time-variant CR distributions) is usually modeled as a Markov deterioration process and is widely used in TAM. By summing up the annual deterioration risks throughout the service life, lifetime risk due to deterioration $R_{L,det}$ can be expressed as follows:

$$R_{L,det} = \sum_{t} \frac{R_{det}(t)}{(1+r)^t}$$

Equation 1.3 Lifetime deterioration risk

where $R_{det}(t)$ = deterioration risk in year t, which is calculated based on the CR distribution in year t using Equation 1.2; r = real annual discount rate. Note that the denominator in Equation 1.3 should be switched to e^{rt} if continuous compounding (instead of annual compounding) is used. This real discount rate is affected by nominal discount rate and expected inflation rate and may theoretically take either positive or negative values. Its value is usually decided by the agency based on different planning horizons. Hence, it is out of the scope of this project. In the following discussion, the real discount rate is assumed to be zero for simplicity. It should also be noted that Equation 1.3 is only valid when the annual failure probabilities are small (as in the case of bridges and tunnels) or the autocorrelation between failures in subsequent years is low. If these conditions are not met, error correction techniques such as those proposed in Yang et al. (2021) can be carried out to improve the estimation of lifetime risk.

1.4 RISK-BASED TRANSPORTATION ASSET MANAGEMENT

Equation 1.3 has important implications for risk-based transportation asset management. It has been shown in existing studies that the minimization of lifetime deterioration risk can be used as a target for planning preservation and maintenance actions (Yang & Frangopol, 2021). The way annual risks are added to determine lifetime risk has also been used to determine risks under extreme events such as earthquakes (Dong, et al., 2015). Hence, the goal of asset management and risk mitigation can be objectively amalgamated as the minimization of total lifetime risk under multiple, deterioration-included hazards. This goal can then be combined with other objectives of transportation asset management, e.g., stabilizing maintenance expenditure over the decision horizon.

However, different from total risks from independent hazards, deterioration may exacerbate the risk of structural failure under extreme events. Specifically, deterioration increases the vulnerability of structures under extreme events, i.e., $p_{DS|IM}(ds|im)$ in Equation 1.1. For instance, corrosion of steel reinforcement and crack/spalling of concrete cover can compromise the seismic resistance of bridge peers (Bhandari 2023). This, in turn, alters the fragility curves associated with different DSs, resulting in changes in $p_{DS|IM}(ds|im)$ during the service life of a structure.

To reflect this interaction, the total risk R_{total} considering deterioration and deterioration-execrated hazards should be expressed as follows:

$$R_{total}(t) = R_{det}(t) + R_{xev}(t)$$

$$R_{det}(t) = \sum_{cr} cq_f \cdot p_f(cr) \cdot p_{CR}(cr|t)$$

$$R_{xev}(t) = \sum_{cr} p_{CR}(cr|t) \cdot \int_{im=a}^{im=b} \left[\sum_{ds} cq(ds)\, p_{DS|IM}(ds|im, cr) \right] |\lambda'_{IM}(im)| dim$$

Equation 1.4 Total risk of two interacting hazards

where $R_{xev}(t)$ = extreme event risk in year t considering structural deterioration. Note that the deterioration risk $R_{det}(t)$ itself is identical to that in Equation 1.2 except that the CR distribution is now explicitly tied to time in service t. The risk due to extreme events $R_{xev}(t)$ considers the impact of deterioration by using additional parameter cr for fragility curves. These time- or condition-dependent fragility curves can yield time- or condition-dependent DS distributions, i.e., $p_{DS|IM}(ds|im, cr)$.

The total lifetime risk, $R_{L,total}$, can be calculated similarly to Equation 1.3 with annual risks calculated using Equation 1.4. This total lifetime risk is important to the framework for risk-based transportation asset management. For instance, consider a time- or condition-based maintenance policy that can improve the CR distribution over the asset service life, i.e., $p_{CR}(cr|t)$. The benefit of that maintenance policy may be quantified by reduced risk that includes both deterioration and extreme event risks. Specifically, for a maintenance policy with a cost of C_{mx}, the benefit-to-cost ratio can be calculated as:

$$\rho_{mx} = \frac{R_{L,total}(na) - R_{L,total}(mx)}{C_{mx}}$$

Equation 1.5 Benefit-to-cost ratio including total lifetime risks

where $R_{L,total}(na)$ and $R_{L,total}(mx)$ = the total lifetime risk without (na) and with maintenance (mx), respectively. If an optimal policy is sought from many candidate actions, the benefit in the numerator in Equation 1.5 can be treated as the objective function of a cost-constrained life-cycle optimization problem.

Overall, this concept of total lifetime risk can benefit transportation asset management in the following aspects:

- It allows for better coordination between condition preservation and risk mitigation activities. For instance, if a more stringent maintenance policy is put in place for bridge substructure, its associated benefit on seismic risk reduction can also be taken into account with Equation 1.5. On the other hand, if seismic retrofitting also enhances the load-carrying capacity for heavy vehicles, the additional benefit of reducing deterioration risk can be quantified as well.
- The risk-based approach facilitates more rational decision-making. Risks from both deterioration and extreme events are objectively assessed and expressed in monetary units

using the risk integral. As a result, it is no longer necessary to subjectively mix performance in condition preservation and benefit of risk reduction for a particular maintenance or retrofitting policy (as it is currently done in most existing BMSs).

1.5 SUMMARY

By treating deterioration as a separate hazard, total lifetime risk from deterioration and extreme events is determined to achieve risk-based transportation asset management. While different from previous methods for considering risks in TAM, the proposed framework relies on objective risk assessment consistent with other frameworks for modeling infrastructure risk and resilience.

Basic ingredients of the risk-based framework are summarized. To estimate deterioration risk, the following data and models are needed:

- *Markov or other deterioration models with respect to asset condition scores such as states, ratings, or health index*. These models are usually available in existing TAM systems.
- *Costs and probabilities of service disruption corresponding to different condition scores*. These probabilities can be inferred from past records of emergency repairs or asset closures. Alternatively, they can be approximated by structural reliability analysis if only severe disruption or structural failures are considered. Future studies are needed to standardize the derivation of these data.

To estimate extreme event risk, necessary data and models include:

- *Hazard characterization curves (i.e., intensity measure vs. annual rate of exceedance).* For earthquake hazards, these can be found from USGS databases. For hydrometeorological hazards, tailored models may be needed to derive these curves, e.g., see HAZUS Flood Model (FEMA 2009) for more details.
- *Sets of fragility curves for different damage states (each set corresponds to a condition score)*. Although several existing studies proposed seismic fragility curves for specific deteriorated bridges and tunnels, there is a lack of widely-applicable fragility curves for deteriorated assets suitable for network-level analysis in TAM. Future studies in these directions are needed.
- *Costs associated with different damage states.* These data are often available in existing risk assessment frameworks (e.g., HAZUS and IN-CORE) and/or obtainable from damage inspection reports and reconnaissance studies.

Finally, it is worth mentioning that the interaction of hazards (similar to that between deterioration and extreme events) may also appear in other settings if one hazard can affect the structural vulnerability under the presence of another hazard. An example of this multi-hazard setting is the total risk from scour and earthquakes, where the scour damage at the foundation can exacerbate structural vulnerability to seismic events. The risk integral of interacting hazards, as determined in this chapter, can facilitate future studies in this direction.

CHAPTER 2

OBJECTIVE RISK ASSESSMENT USING WEIGHTED HAZARD SCENARIOS

2.1 INTRODUCTION

The framework for risk-based transportation asset management hinges on the objective risk assessment under deterioration and extreme events. As described in Chapter 1, the risk of critical transportation assets should be objectively expressed as a risk integral (i.e., Equation 1.1), considering quantified uncertainties arising from hazard characteristics, structural vulnerability, and damage consequences. However, the evaluation of a risk integral differs considerably from the estimation of risk in most existing TAM systems, hindering its application in bridge and tunnel management. For existing methods compatible with or potentially applicable to bridge management systems (BMSs), risks are usually estimated following the general procedure outlined below (Western et al. 2016; AASHTO 2021):

(a) *Collect one or a limited number of hazard scenarios relevant to the asset performance.* These are usually obtained from expert elicitation or past experience. They can be different hazards (e.g. earthquakes and floods), one hazard with different return periods (thus different intensity levels), or one hazard with a specific return period causing a particular damage extent (in term of a DS).
(b) *Estimate the annual rate of each hazard scenario*. This can be determined from polls on experts or past experience of agencies. Results of probabilistic hazard analysis, e.g., those available through USGS for earthquakes, can also be utilized in this step.
(c) *Estimate the expected consequence under each hazard scenario.* This can be similarly determined from expert polls or past experience. Alternatively, damage evaluation given the scenario event can be conducted using HAZUS or in-house tools (FEMA 2023; Western et al. 2016). Note that this differs from a risk analysis as it assumes that the hazard event will occur and calculates the expected cost considering only the uncertainties in structural vulnerability.
(d) *Tabulate the risks associated with all hazard scenarios* by multiplying the annual rates and the expected consequences. *Sum up the risks of hazard scenarios* as the total annual risk associated with the asset. Tally all annual risks to *determine the lifetime risk.*

Table 2.1 presents a generic example of this approach to computing seismic risk (hereafter referred to as the BMS approach[1]). Despite the noticeable differences in formulations, the BMS approach can be interpreted as a numerical integration procedure (i.e., using the rectangular rule) for the risk integral in Equation 1.1. This is achieved by substituting the integration along the continuous intensity measure with a summation over all scenario events, shown as follows:

[1] Note that this refers to existing methods within the reasonable capability of modern BMS implementations.

$$R = \int_{im} \left[\sum_{ds} cq(ds) \cdot p_{DS|IM}(ds|im) \right] |\lambda'_{IM}(im)| dim$$
$$\approx \sum_{im_{ev}} \overline{CQ}(im_{ev}) \cdot v_{IM}(im_{ev})$$

Equation 2.1 Risk approximation implied in the BMS approach

where $\overline{CQ}(im_{ev}) \equiv \sum_{ds} cq(ds) \cdot p_{DS|IM}(ds|im_{ev})$ = expected consequence under a hazard scenario with an intensity level equal to im_{ev}; $v_{IM}(im_{ev})$ = annual rate of the hazard scenario, which can be approximated by the difference between the annual exceedance rate between one hazard scenario and the next more severe hazard scenario. For instance, the rate of a 225-year earthquake in Table 2.1 is the difference between 1/225 and 1/975, the annual exceedance rate of the next hazard scenario (i.e., a 975-year earthquake).

Table 2.1 Tabulation approach to risk estimation in common BMSs

Hazard Scenario	Description	Annual rate	Intensity[a] (PGA, *g*)	Consequence[b] (cost ratio)	Risk (cost ratio)
1	225-year earthquake	3.418×10^{-3}	(0.407)	0.326	1.114×10^{-3}
2	975-year earthquake	6.220×10^{-4}	(0.774)	0.691	4.298×10^{-4}
3	2475-year earthquake	4.040×10^{-4}	(1.017)	0.819	3.309×10^{-4}
				Total risk	1.875×10^{-3}

Notes:

(a) This column contains intensity measures in terms of PGA (in unit g). The values are in parentheses because they are not directly used by BMSs. Instead, they are used to determine the damage state probabilities and the expected damage consequence of a hazard scenario.

(b) Values in this column are expressed as cost ratios, i.e., the ratio of repairing to rebuilding costs.

Subjectivity of this BMS approach can arise from the subjective selections of hazard scenarios and assignments of their annual rates and consequences. This subjectivity can be partially alleviated by using probability hazard analysis for step (b) and using structural fragility analysis for step (c), as implemented in Table 2.1. However, the selection of hazard scenarios remains a major hinderance to objective risk assessment. Additionally, an accurate estimation of an integral with the rectangular rule demands a large number of hazard scenarios, which are usually not practical in BMS implementations. We demonstrate in the later sections that the tabulation approach based on a few subjectively selected hazard scenarios cannot accurately estimate the risk integral. To overcome this challenge, a novel tabulation approach based on weighted hazard scenarios is described.

2.2 RISK ASSESSMENT USING WEIGHTED HAZARD SCENARIOS

A new tabulation method is developed herein by leveraging a more accurate and efficient numerical integration method, i.e., the Gaussian quadrature method, in place of the rectangular rule implied in the current BMS method. The objectives of this new method are as follows:

- Reduce the number of hazard scenarios needed to accurately estimate the risk integral;

- Preserve the general implementation steps for easy integration with existing BMSs.

The mathematical formulation of the Gaussian quadrature method for numerical integration is provided in Appendix A. Figure 2.1 illustrates the concept underpinning the Gaussian quadrature method for numerical integration. Figure 2.1(a) shades the region under the multiplication of the likelihoods and the consequences for different intensity levels. The risk integral is, therefore, the area of the shaded region. Figure 2.1(b) illustrates the use of Equation 2.1 for approximating this integral. As shown in Figure 2.1(c), the Gaussian quadrature method strategically selects the location (highlighted dots in the figure) and the weights of intensity levels (width of the rectangles in the figure) so that the sum of the shaded areas can be better estimated with the same number of intensity levels. Applying the Gaussian quadrature method to the risk integral in Equation 1.1 gives rise to the following equation:

$$R = \int_{im=a}^{im=b} \left[\sum_{ds} cq(ds) \cdot p_{DS|IM}(ds|im) \right] |\lambda_{IM}{}'(im)| dim$$
$$\approx \sum_{i=1}^{n} \underbrace{w_i}_{weight} \cdot \underbrace{\left[\sum_{ds} cq(ds) \cdot p_{DS|IM}(ds|im_i) \right]}_{expected\ \ conse\ quence} \cdot \underbrace{v_{IM}(im_i)}_{nominal\ \ rate}$$

Equation 2.2 Risk calculation with numerical integration (Gaussian quadrature)

where w_i = weight of the ith scenario event, equal to the integration weight η_i of the ith Gaussian integration point (see Appendix A for more details). The summation in Equation 2.2 can be treated as the total risk from n scenario events, each with a unique intensity level im_i and responsibility weight w_i to the total risk. Equation 2.2 slightly differs from Equation 2.1 in the following two aspects: (a) the introduction of responsibility weights assigned to different scenarios and (b) the determination of the annual rate of occurrence for a scenario event. This nominal annual rate of occurrence, $p_{IM}(im_i)$, is calculated as follows:

$$v_{IM}(im_i) = \frac{b-a}{2} |\lambda_{IM}{}'(im)|$$

Equation 2.3 Nominal annual rate of occurrence

Due to the similarity between Equation 2.1 and Equation 2.2, the numerical integration represented by Equation 2.2 can be directly implemented using the same steps described in Section 2.1 and a similar table to Table 2.1 after (a) scaling the expected consequences with the responsibility weights and (b) replacing the annual rates with $v_{IM}(im_i)$ for all scenarios. The new method represented by Equation 2.2 is referred to herein as the method of risk assessment using weighted hazard scenarios.

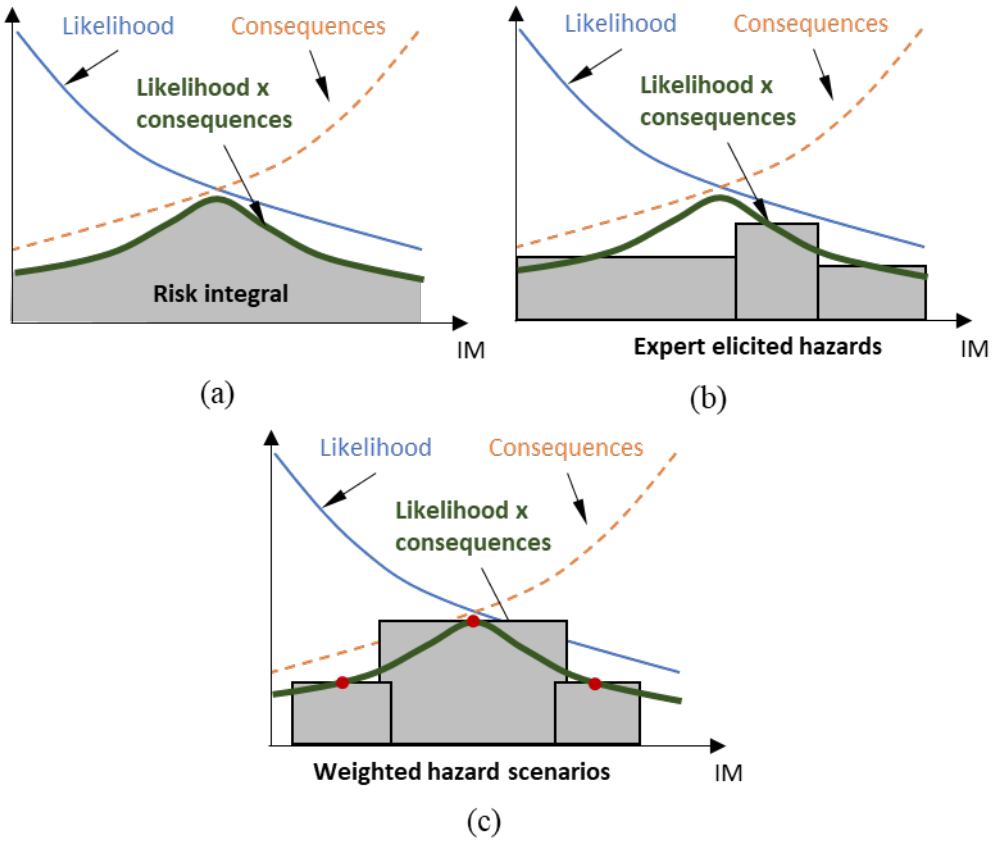

Figure 2.1 Concept of Gaussian quadrature for numerical integration: (a) precise risk integral, (b) risk estimated by expert elicitation, and (c) weighted hazard scenarios from Gaussian quadrature

In Equation 2.2, the integration domain $[a, b]$ can be regarded as the intensity levels responsible for the asset risk under adverse events. For instance, a domain [0.1g, 2.0g] for peak ground acceleration (PGA) may be used for estimating asset seismic risk if (a) an asset is extremely unlikely to damage with PGA less than 0.1g and (b) an earthquake causing PGA larger than 2.0g is extremely unlikely to happen in the region (and a lower PGA already causes catastrophic consequences). This domain is responsible for determining the intensity levels im_i of different hazard scenarios, as specified by the following equation:

$$v_{IM}(im_i) = \frac{b-a}{2}|\lambda_{IM}{}'(im)|$$

Equation 2.4 Scenario weights and intensity levels

where ξ_i = integration points given a n-point Gaussian quadrature. As discussed in Appendix A, once the number of hazard scenarios (i.e., the integration points n) are selected, η_i and ξ_i are predetermined and do not depend on the integrand function in Equation 2.2. Nonetheless, the number of hazard scenarios itself that can yield accurate estimation does hinge on the integrand function. In practice, this number can be raised incrementally until the estimated risk converges.

Through numerical examples in later sections, it will be shown empirically that risk assessment using weighted hazard scenarios is accurate with only a small number of scenarios.

To facilitate the application of this new approach, a Python package named pyRiskTable has been developed to automatically generate a comma-separated values (CSV) file containing weighted hazard scenarios given a target accuracy level. Figure 2.2 illustrates the basic components of this package and their relationships. The package is available as a code repository on GitHub[1] at https://github.com/cedavidyang/risk-based-BMS.git. We will grant access to the package upon request. It is our intention to open-source this package once the review is complete and the package is out of its beta stage.

[1] The U.S. Government does not endorse products or manufacturers. They are included for informational purposes only and are not intended to reflect a preference, approval, or endorsement of any one product or entity.

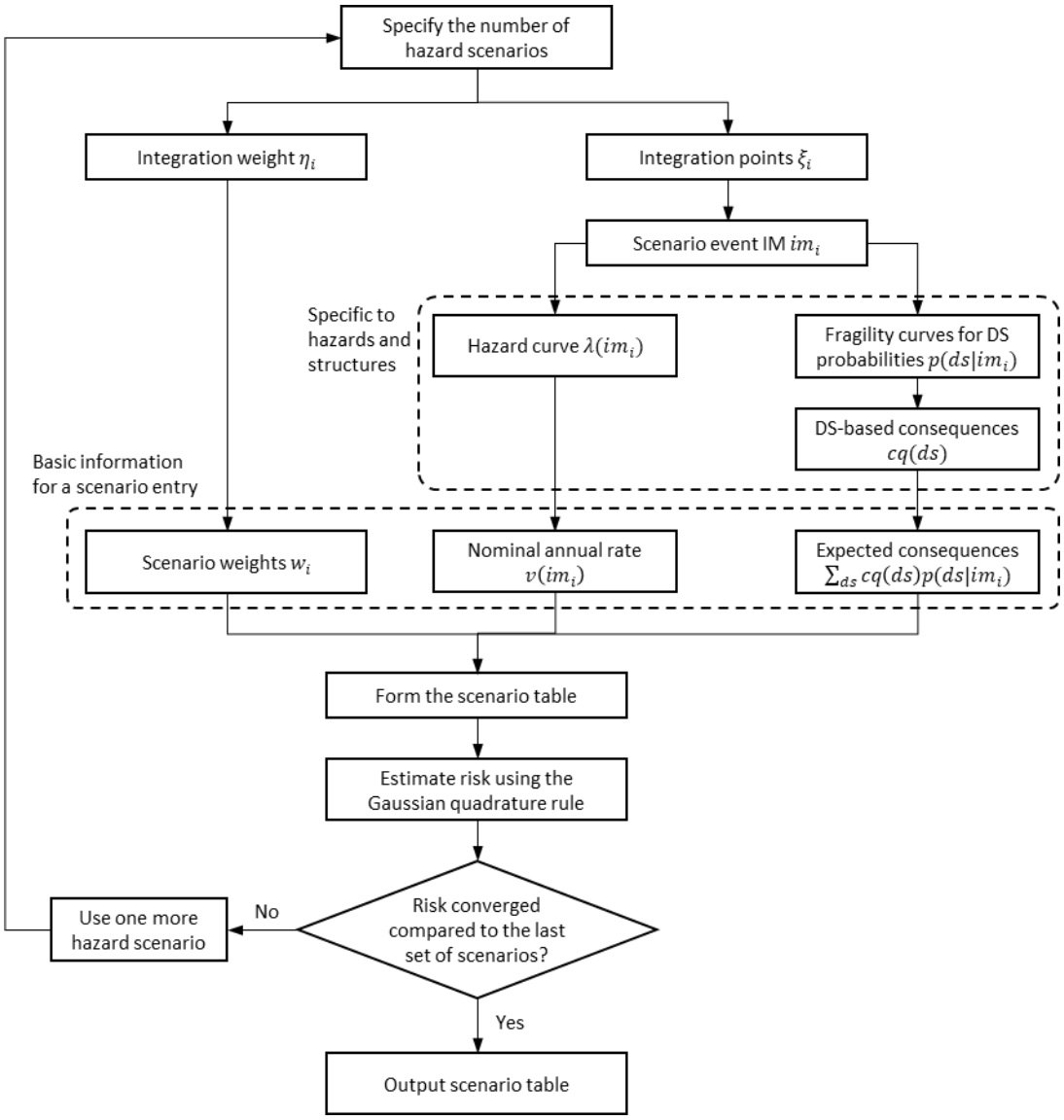

Figure 2.2 Flowchart of the developed package (pyRiskTable)

2.3 WEIGHTED HAZARD SCENARIOS FOR DETERIORATING ASSETS

During the service life of an asset, deterioration may affect its vulnerability under extreme events. For instance, as mentioned in Chapter 1, deterioration can amplify seismic fragility. Therefore, it is important to use age- or condition-dependent fragility curves to reflect the effect of deterioration (Muntasir Billah & Shahria Alam 2015). This change in fragility curves affects the expected consequences determined by Equation 2.2. If the probability distribution of damage states (DSs) is linked to time in service, the expected consequence also becomes age-dependent, as represented by the following equation:

$$\overline{CQ}(im|t) = \sum_{ds} cq(ds) \cdot p_{DS|IM}(ds|im,t)$$

Equation 2.5 Expected consequence based on age-dependent fragility curves

where $p_{DS|IM}(ds|im,t)$ = probabilities of different DSs after t years in service if a hazard with intensity level im occurs in year t. These probabilities should be determined based on age-dependent fragility curves. Alternatively, if the effect of deterioration on extreme event risk is reflected by condition-dependent fragility curves, the expected consequence can be formulated by rearranging Equation 1.4 as follows:

$$\overline{CQ}(im|t) = \sum_{cr} p_{CR}(cr|t) \cdot \sum_{ds} cq(ds)\, p_{DS|IM}(ds|im,cr)$$

Equation 2.6 Expected consequence based on condition-dependent fragility curves

Equation 2.5 and Equation 2.6 indicate that the integrand of the risk integral varies within the asset service life due to deterioration. Because of this change, weighted hazard scenarios should be, in principle, regenerated every year in the asset service life to ensure that the annual risk can be accurately estimated. However, this regeneration can significantly complicate the implementation in existing BMSs.

In the later section, the error of keeping the same set of weighted hazard scenarios (derived from the fragility model of a pristine asset without deterioration) will be investigated through a numerical example. Specifically, it will be shown that even under extreme deterioration that may not be realistically experienced in civil structures, the error introduced by using a fixed set of hazard scenarios is not significant. Hence, the method based on weighted hazard scenarios can also be used for risk assessment of deteriorating assets under extreme events.

2.4 ILLUSTRATIVE EXAMPLE

The approach described in the previous section is illustrated herein by an example focusing on bridge seismic risk assessment. The flowchart in Figure 2.2 is used to derive the weighted hazard scenarios. The result is compared in terms of accuracy to the existing tabulation approach in BMSs. This example is then leveraged to illustrate implications of objective risk assessment on the life-cycle management of deteriorating assets.

2.4.1 Hazard Characteristics, Bridge Fragility, and Damage Consequences

In this example, a fictional hazard curve based on an idealized fault 10 km away from the site is considered following Baker (2013). The fault is assumed to only generate magnitude 6.5 earthquakes with a return period of 100 years. Using probabilistic seismic hazard analysis, the following hazard curve can be derived (Cornell et al. 1979; Baker 2013):

$$\overline{ln\, PGA} = -0.152 + 0.859M - 1.803\, ln(d + 25)$$

$$\lambda_{IM}(im) = 1 - \Phi\left(\frac{ln\, im - \overline{ln\, PGA}}{\sigma}\right)$$

Equation 2.7 Hazard curve

where M = magnitude of the earthquakes generated at the fault ($M = 6.5$ in this example); d = distance between the site and the fault in kilometers ($d = 10$ km in this example); Φ = cumulative distribution function (CDF) of a standard normal distribution; σ = dispersion factor of the PGA (i.e., the standard deviation of the logarithmic PGA) at the site, and $\sigma = 0.57$ is assumed herein (Cornell et al. 1979). This hazard curve gives the annual rate of exceedance $v_{IM}(im)$ under different PGA levels. Both the hazard curve and its gradient with respect to PGA are shown in Figure 2.3. It should be noted that the hazard curve has a maximum annual rate of exceedance of 0.01 due to the assumed return period of earthquakes at this idealistic fault.

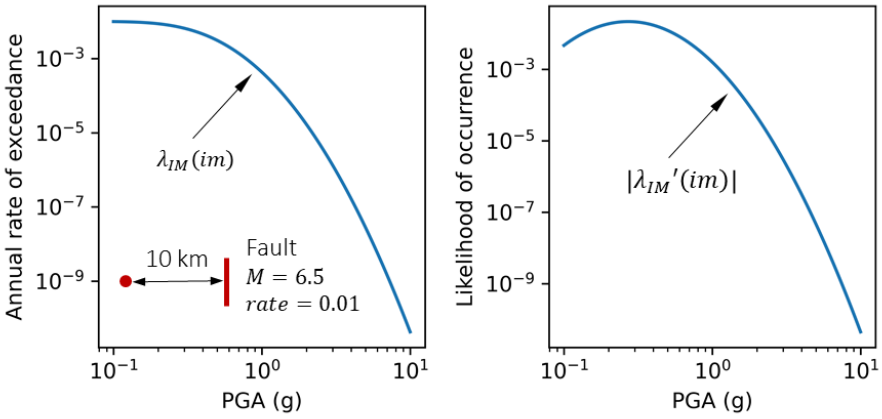

Figure 2.3 Hazard curve and the absolute value of its gradient

Fragility curves in Basöz and Mander (1999) are used to determine the DS probabilities given an intensity level at the site. For each DS, the fragility curve is modeled by the CDF of a two-parameter lognormal distribution, median PGA and the dispersion factor (i.e., the standard deviation of $\ln PGA$). Table 2.2 gives the two parameters used for each DS. The DS probability can be determined by comparing the fragility curves between two consecutive DSs, as illustrated in Figure 2.4.

Table 2.2 Fragility curve classification

Damage state	Median PGA (in g)	Dispersion ($\sigma_{\ln PGA}$)
Slight	0.30	0.6
Moderate	0.36	0.6
Extensive	0.49	0.6
Complete	0.71	0.6

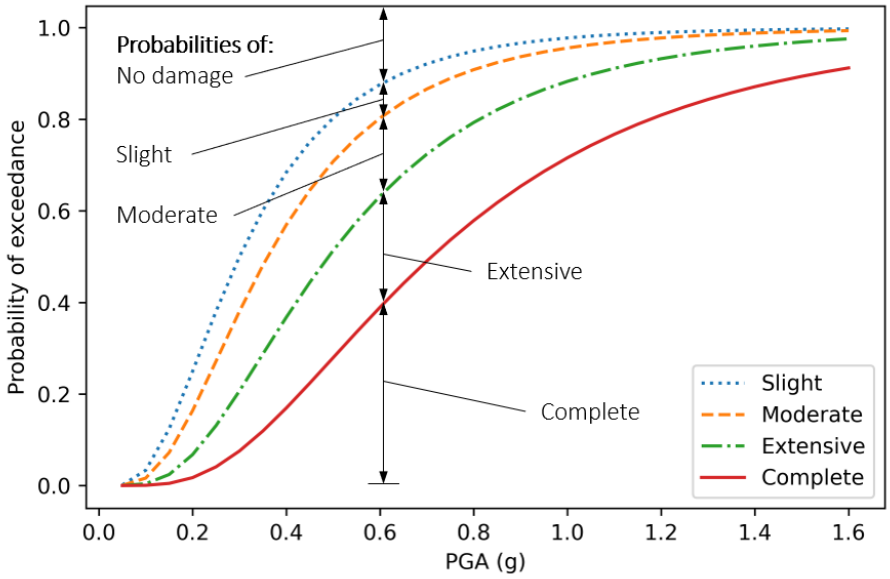

Figure 2.4 Fragility curves and damage state probabilities

It is worth mentioning that the fragility curves in Figure 2.4 use PGA as the intensity measure, which allows us to directly connect the fragility curve with the results from probabilistic seismic hazard analysis. Although the curves presented herein were used to derive the HAZUS fragility models, HAZUS has since switched to spectral acceleration (SA) as the intensity measure. The conversion from PGA to SA can be found in Basöz and Mander (1999). For the convenience of the analysis herein, this conversion is not implemented.

Lastly, damage state consequences are described in terms of cost ratios, calculated as the ratio of damage cost to replacement cost. Table 2.3 presents these cost ratios based on the data from past field studies and summarized in Basöz and Mander (1999).

Table 2.3 Average cost ratios for different damage states

Slight	Moderate	Extensive	Complete
0.12	0.19	0.48	1

2.4.2 Seismic Risk Assessment with Weighted Hazard Scenarios

The Python-based tool described in Section 2.3 is used to generate weighted hazard scenarios, based on which the seismic risk of the bridge can be computed with the tabulated sum. Following the flowchart in Figure 2.2, a threshold of 0.05 is used to determine the appropriate number of weighted hazard scenarios, namely, the hazard number keeps increasing until the risks estimated between two consecutive iterations are less than 5% apart. To avoid premature stopping of this iterative process, at least four scenarios are needed for the risk estimation. Additionally, the

integral domain is selected based on the lower and upper limits of intensity levels that correspond to two return periods, namely 100 years[1] and 100,000 years.

Based on these parameters, six hazard scenarios are obtained. Table 2.4 presents the intensity measures, event rates (nominal), scenario weights, and damage consequences for all six scenarios. Also included in the table are the return periods for all events backcalculated from the intensity levels. It should be noted that these return periods are not needed in the new approach. They are presented herein to showcase the consistent format of the new approach compared to the BMS method currently in use. By tabulating the weighted risks of these scenarios (calculated as the product of the rate, consequence, and weight), the total seismic risk is 0.00340 (in terms of cost ratio). This is very close (within 2% margin) to the precise value of the risk integral (0.00332) evaluated based on Equation 1.4 with numerical integration.

Table 2.4 Weighted hazard scenarios and risks

Hazard scenario	Description (return period, PGA in g)	Annual rate	Consequence (cost ratio)	Weight	Risk (cost ratio)
1	104 yr, PGA=0.136	1.119E-02	0.021	0.171	4.078E-05
2	240 yr, PGA=0.424	1.712E-02	0.348	0.361	2.148E-03
3	1435 yr, PGA=0.873	2.855E-03	0.752	0.468	1.004E-03
4	8873 yr, PGA=1.379	3.991E-04	0.916	0.468	1.711E-04
5	36247 yr, PGA=1.828	8.597E-05	0.966	0.361	2.995E-05
6	82265 yr, PGA=2.116	3.502E-05	0.980	0.171	5.879E-06
				Total risk	**0.00340**

To demonstrate advantages over the existing approach, six typical hazard scenarios are utilized to estimate the risk with the BMS/NCHRP approach. The return periods of these scenarios are selected because they are commonly used in either expert-based seismic risk assessment or seismic analysis and design of structures. Table 2.5 presents the return periods, corresponding event rates, implied intensity levels, and damage consequences of all scenarios. The risks associated with the scenarios and the total risk are also presented in Table 2.5. It can be observed that the total risk obtained from the BMS approach underestimates the precise risk by 36% (0.002117 vs. 0.00332).

Table 2.5 Risk assessment based on BMS procedures

Hazard scenario	Description (return period, PGA in g)	Annual rate	Consequence (cost ratio)	Risk (cost ratio)
1	225 yr, PGA=0.326	2.444E-03	0.326	7.958E-04
2	500 yr, PGA=0.554	9.740E-04	0.554	5.397E-04
3	975 yr, PGA=0.691	3.590E-04	0.691	2.480E-04
4	1500 yr, PGA=0.758	1.670E-04	0.758	1.266E-04
5	2000 yr, PGA=0.795	9.600E-05	0.795	7.633E-05
6	2475 yr, PGA=0.819	4.040E-04	0.819	3.309E-04
			Total risk	**0.002117**

[1] For implementation, 100.01 years is used as the lower limit to avoid numerical issues that arise when 100 years is plugged into the hazard curve to derive the corresponding intensity level.

Based on the similar format between Table 2.4 and Table 2.5 , it is clear that the new approach can be directly integrated into existing BMSs without significantly altering the current workflow of transportation asset management. Specifically, an analyst only needs to combine the scenario weights with the scenario consequences and feed the scaled consequences to BMSs together with the event rates to achieve objective risk assessment.

2.4.3 Seismic Risk of Deteriorating Bridges

Since the hazard curve in Figure 2.3 describes the annual rate of exceedance, the risk value previously computed represents the annual seismic risk of the bridge. With deterioration, the seismic fragility curves may change over time. Herein, an age-dependent model for fragility curves is assumed to investigate the accuracy of the estimated risk using the same set of weighted hazard scenarios in Table 2.4 through the bridge service life[1]. Specifically, the median PGA value of a fragility curve (related to the seismic resistance of a bridge) is assumed to decrease over time in the following fashion:

$$r^{(ds)}(t) = \frac{PGA_m^{(ds)}(t)}{PGA_m^{(ds)}(0)} = 1 - at$$

Equation 2.8 Time-dependent seismic performance considering deterioration

where $PGA_m^{(ds)}(0)$ and $PGA_m^{(ds)}(t)$ = median PGAs, associated with damage state ds, at the start of the service life (pristine state) and after t years in service, respectively; a = annual deterioration rate. Herein, a linear relationship with respect to time is used for simplicity. It is assumed herein that $a = 0.01$. Since the median PGA is approximately the square root of the seismic resistance (Basöz & Mander 1999), the assumed deterioration rate implies that by the end of a 75-year service life, the median PGA reduces to 25% of its initial value, corresponding to a 93.75% ($= 1 - 25\%^2$) decrease in seismic resistance. This is, thus, a conservative estimation of the deterioration extent. If the error in risk does not increase significantly under this extreme deterioration condition, it can be safely concluded that the error is negligible under more realistic deterioration conditions.

To verify the applicability to deteriorating assets, the risk integral associated with a bridge that deteriorates following Equation 2.8 is evaluated for each year in service with two methods. For the first method, the same hazard scenarios as those in Table 2.4 are adopted. In particular, annual rates and weights are directly obtained from Table 2.4 for all years in service. The effect of deterioration is reflected by the age-dependent expected consequences calculated with Equation 2.5 and Equation 2.8. For the second method, the precise risk value in each year is directly computed using Equation 1.1 and numerical integration. Figure 2.5 shows the seismic risk profile in the 75-year service life using both methods. The difference between the two profiles represents the error in risk assessment when using the same set of weighted hazard scenarios derived from

[1] Note that the expected consequences may change over time and will be updated using age-dependent fragility curves. However, the number of hazards and the hazard intensity levels are not changed throughout the service life.

the pristine bridge. The relative error is also plotted in Figure 2.5. It can be observed that using the same set of weighted hazard scenarios does not substantially compromise the accuracy of risk estimation. In fact, even at the end of the service life, when deterioration is extremely severe, the relative error is still below 5%. As discussed previously, the results indicate that the initial weighted hazard scenarios are effective in assessing extreme event risk of deteriorating assets throughout their service life.

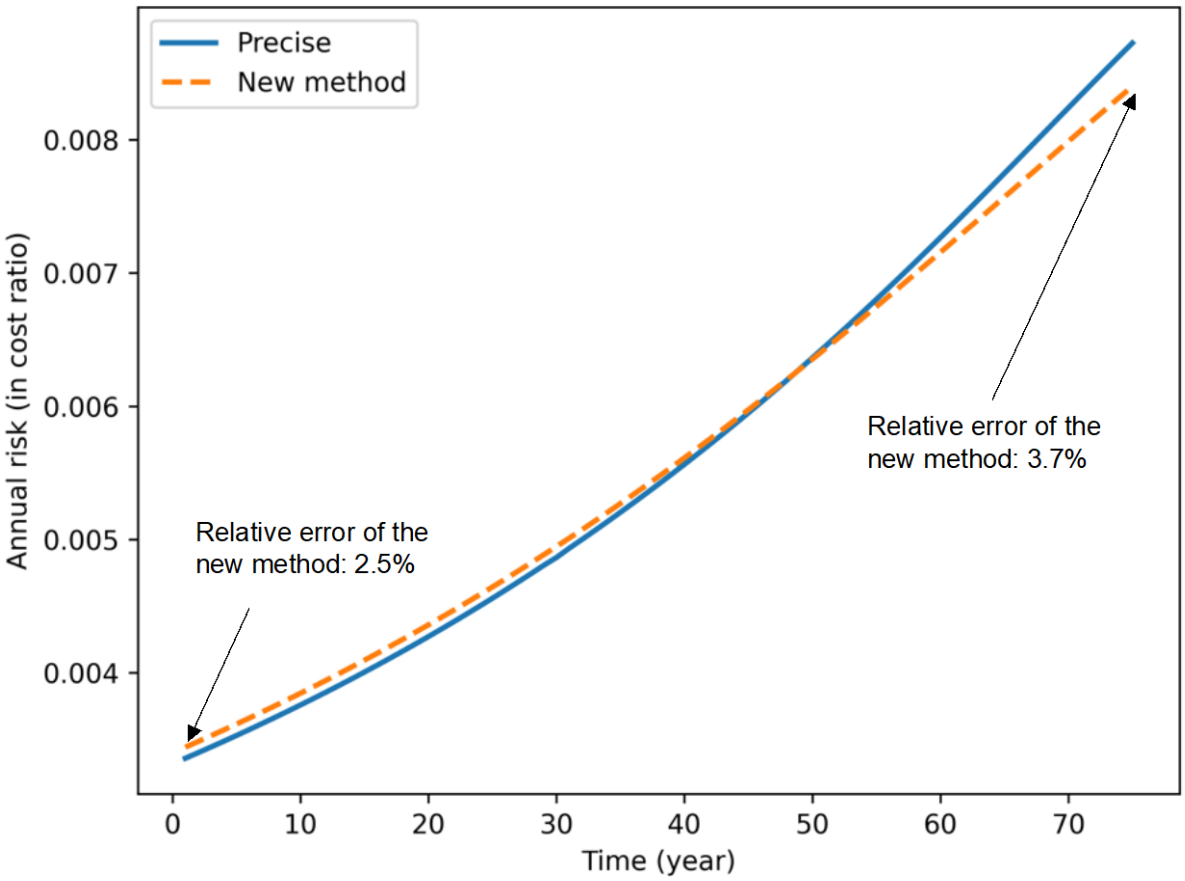

Figure 2.5 Error of using the same set of hazard scenarios for deteriorating assets

2.4.4 Implications of Objective Risk Assessment on Asset Management

One of the primary goals of risk assessment is to carry out risk-based transportation asset management. For instance, different maintenance or retrofitting strategies can be compared based on their benefit-to-cost ratios (BCRs) from Equation 1.5, where the benefit is the reduction in risk attributed to maintenance or retrofitting actions. Therefore, objective and accurate risk assessment has direct implications on BCR calculation. To illustrate the implications of this method to TAM, the following two fictional maintenance strategies are considered:

- Strategy 1: Maintain the bridge every two years to immediately rectify any deterioration accumulated in the two-year interval and restore the structure to its initial performance.

- Strategy 2: Only provide one major maintenance in year 40 within the 75-year service life to fix the deterioration accumulated in the first 40 years and restore the structure to its initial performance.

The cost of a maintenance action is assumed to be proportional to the extent of performance improvement when the action is taken. Similar to Equation 2.8, the structural performance is expressed as the median PGA (a parameter of a fragility curve related to the seismic capacity) normalized by the initial median PGA (when no deterioration is present). The cost ratio associated with a maintenance action is assumed equal to $1 - r$ where r is the structural performance considering deterioration according to Equation 2.8.

Based on this cost model, the BCRs of both strategies are evaluated using Equation 1.5. The example herein is focused on the additional benefit of maintenance actions in reducing extreme event risks. Therefore, only the lifetime seismic risk (expressed in the last equation in Equation 1.4) is considered to calculate the benefit of a strategy. Additional benefit in reducing deterioration risk is neglected. Following this consideration, the benefit of a strategy is the lifetime seismic risk given the maintenance strategy subtracted from the lifetime seismic risk without maintenance. Annual seismic risks are estimated using Table 2.4 and Table 2.5 for the weighted hazard scenarios method and the BMS/NCHRP approach, respectively. To focus on the implications of risk assessment approaches, the same age-dependent fragility curves expressed in Equation 2.8 are used in both approaches to calculate the age-dependent expected consequences.

Figure 2.6 shows the results of BCR comparison. It can be observed that when the approach for objective risk assessment is used, Strategy 2 is clearly more advantageous than Strategy 1, with an approximately 8% higher BCR. On the other hand, when the BMS approach is used, the difference between the two strategies is negligible, which can complicate the decision-making process. Additionally, the BCR is significantly underestimated when using the existing BMS approach. Hence, inaccurate risk assessment with the existing BMS approach may lead to erroneous ranking of different maintenance or retrofitting strategies. The objective risk assessment provides a viable rectification for this drawback.

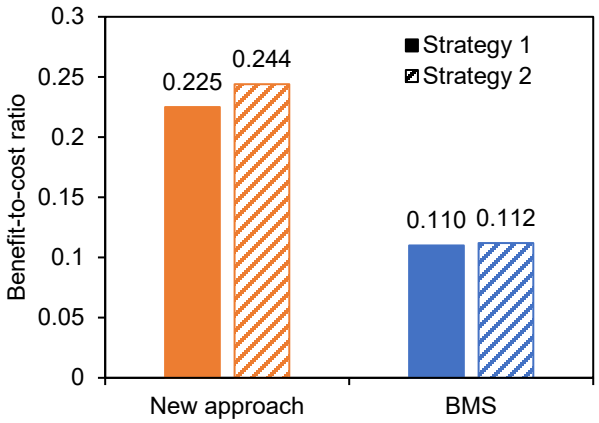

Figure 2.6 BCR comparison of different risk assessment approaches[1]

2.5 SUMMARY

The risk assessment approach based on weighted hazard scenarios is a novel method to potentially fill the gap between risk assessment and asset management. Rather than rely on expert elicitation for hazard scenarios, the new approach for objective risk assessment can automatically and consistently generate weighted hazard scenarios to be included in the risk analysis. The new approach is built on the rigorous formulation of risk integrals and is applicable to both individual hazards and interacting hazards such as those coupled with structural deterioration. The preservation of a tabulated implementation allows for the direct integration of objective risk assessment in common asset management frameworks, laying the foundation for risk-based transportation asset management. It is most convenient to apply the new approach as a pre-processing step when setting up the risk assessment task within common BMSs. Full integration with BMSs (as a built-in feature) is possible, but may need additional coordination and collaboration with software vendors.

In summary, the following conclusions can be drawn:

- Compared to existing risk assessment methods in BMSs, the new approach can yield much higher accuracy with the same number of hazard scenarios. The format of the generated scenarios is similar to that used in BMSs except for a weighting factor that can be merged to event consequences. As a result, the generated hazards can be directly leveraged by existing BMSs to achieve object risk assessment.
- The new approach can handle the interaction between structural deterioration and extreme event risk. It is shown empirically that the same set of weighted hazard scenarios generated for a pristine structure (specifically, the event rates and the responsibility weights) can be used over the entire service life of a structure without introducing notable errors in risk assessment. Nonetheless, the deterioration effect should be reflected by the time-variant expected consequences given hazard occurrences in different points-in-time of the service life.

[1] It should be noted that both strategies have a low BCR. This is due to (a) the neglect of benefit in reducing deterioration risks, (b) the narrow consideration of economic consequences to bridge owners, and (c) the relatively low recurrence rate and magnitude of earthquakes along the assumed fault.

- It is also empirically demonstrated that existing approaches to risk assessment compatible with BMS implementation do not always deliver reliable rankings of maintenance strategies in terms of risk-based benefit-to-cost ratios. This means that the lifetime risk of deteriorating assets cannot be assessed by simply incorporating age- or condition-dependent fragility curves to BMSs. Instead, the new approach to picking hazard scenarios is a necessary step toward risk-based transportation asset management.

CHAPTER 3

MOBILITY RISK ASSESSMENT FOR LARGE-SCALE TRANSPORTATION NETWORKS

3.1 INTRODUCTION

The previous chapter presents an effective and practical approach to objectively assessing asset risks under extreme events, especially when they are also coupled with asset deterioration. The consequence indicators used therein (e.g., cost ratios) indicate that the risk evaluated is primarily direct economic risk to asset owners. One convenient property about agency risk is that the risks from individual assets can be directly added to determine the total risk of a portfolio of transportation assets (Western et al. 2016). This type of risk is termed herein as "additive risk".

Apart from direct economic risks, transportation systems also carry important societal functions prior to, during, and after extreme events, including accessibility to critical public services, capacity for vacation and emergency response, and travel cost of road users, among others. These indirect consequences of asset failure may demonstrate the so-called "network effect": this is where the combined impact of multiple assets failing at once is greater than the total impact of each asset failing individually. This network effect arises primarily due to the interdependency of assets in an interconnected network such as transportation systems (Yang & Frangopol 2018; Yang & Frangopol 2020). These indirect risks are referred herein as the network risk.

For indirect consequences, several performance indicators can be applied, including network connectivity, travel cost, and network capacity (Chang et al. 2012). Connectivity is efficient to compute and especially useful to risk assessment related to life safety when isolated communities without accessibility post-hazard should be minimized through mitigation measures or quickly identified immediately after hazard occurrence. However, connectivity does not cover the full range of transportation performance, especially that related to the mobility of people and goods. For instance, although the connectivity is still available, if the traffic flow capacity is drastically reduced, both emergency response and post-hazard recovery can be negatively impacted.

Travel costs, e.g., total travel time and total travel distance (Ghosn et al. 2016), consider both the capacity of a transportation network and the demand of road users within the network. It provides a complete view of the transportation performance before, during, and after a hazard. However, the computation of travel costs involves solving a traffic assignment problem (Patriksson 2015), which can be computationally expensive for a large-scale network (e.g., at the state level). This computational challenge is further compounded by the need for repeated travel cost evaluations during risk assessment. Additionally, traffic demand can be difficult to estimate far into the future or immediately after a major hazard, making travel cost a less viable performance indictor for life-cycle planning or risk assessment under extreme events.

In this project, we focus on the network capacity as the performance indicator for indirect risk assessment. Network capacity measures the total traffic flow that can be maximally accommodated between all or important origin-destination (OD) pairs in a transportation network (Morlok & Chang 2004). It is an intrinsic characteristic of a network that is independent of traffic demand but is sensitive to the capacity of each link and how these links are connected in a network. Therefore,

network capacity is considered a "middle ground" between connectivity and travel cost (Chang et al. 2012). On the one hand, the network capacity automatically reflects connectivity issues, which can be manifested as a zero capacity between an OD pair. On the other hand, network capacity bypasses the need for demand estimation, thereby avoiding the shortcomings of travel cost evaluation. However, it can still implicate mobility issues that are usually at least partially attributed to insufficient road capacities. Additionally, network capacity can be computed very efficiently even for large-scale transportation systems.

Based on network capacity, the network risk ρ_{NET} of a transportation system can be expressed as (Yang & Frangopol 2020; Yang 2022):

$$\rho_{NET} = \sum_{\boldsymbol{s}} p(\boldsymbol{s}) \cdot \left| C_{NET}(\boldsymbol{s}) - C_{NET,0} \right|$$

Equation 3.1 Expression of network risk

where $p(\mathbf{s})$ = probability of the system state $\mathbf{s}$; $C_{NET}(\mathbf{s})$ = system-level consequences given the system state $\mathbf{s}$; $C_{NET,0}$ = system-level consequences without any damage, respectively. It should be noted that the probability $p(\mathbf{s})$ can represent system damage under both an extreme event and/or deterioration. For the latter, the damage to the system can be calculated as the deterioration-induced service disruption of one or multiple assets within a specific year in the service life[1]. On the consequences side, different from direct economic risk, capacity-based network risk does exhibit the network effects. Therefore, the evaluation of system-level consequences in Equation 3.1 calls for the complete knowledge of all asset conditions. To calculate the network capacity, Appendix B provides detailed information on how transportation systems can be modeled as graphs and how the network capacity can be evaluated rigorously using this graph model.

For a large-scale transportation system with hundreds to thousands of assets, assessing the network risk is extremely complicated due to the enormous amount of unique system states. For instance, if we consider two states for each asset (e.g., complete damage and survival), a system made up of 100 assets gives rise to $2^{100} - 1 \approx 10^{30}$ unique system states with failure consequences. This number renders precise evaluation using Equation 3.1 impractical. Since the state of each asset can be regarded as a random variable influencing the network risk, the challenge of risk assessment for a large-scale system is also referred to as the challenge of risk assessment in high dimensions (or in high-dimensional space). In this chapter, a more effective and efficient algorithm based on Transitional Markov chain Monte Carlo (TMCMC) is selected to overcome this computational challenge related to network risk assessment.

3.2 EFFICIENT ALGORITHM FOR LARGE-SCALE NETWORK RISK ASSESSMENT

Due to the challenge mentioned above, previous approaches to network risk assessment have primarily dealt with small- to moderate-scale systems with dozens of assets (Saydam et al. 2013;

[1] The risk within multiple years can then be approximated by the sum of annual risks.

Bocchini & Frangopol 2011; Yang & Frangopol 2020; Yang & Frangopol 2019; Yang & Frangopol 2018; Bensi et al. 2015). At those scales, network risk can be analytically bounded using a subset of all system states, e.g., by considering the system states with up to a specific number of damaged assets (Yang & Frangopol 2019). However, for large-scale systems, risk can no longer be effectively bounded in this manner.

Often, Monte Carlo (MC) simulation, which randomly samples system states and evaluates the corresponding consequences, becomes the last resort (Rokneddin et al. 2014; Vishnu et al. 2023). However, conventional MC simulation tends to concentrate the sampling effort on the system states with high likelihood of occurrence. Due to the large number of system states, it becomes challenging to sample system states that have low likelihood of occurrence but high consequences, i.e., the so-called "grey swan" events[1]. As a result, MC simulation may perform poorly for network risk assessment when/if the risk is heavily influenced by "grey swan" events.

To overcome the shortcomings of existing methods, a novel sampling method based on TMCMC is developed and described in detail in this section. Specifically, the risk determined by Equation 3.1 is first formulated as an integral with respect to a multivariate normal distribution. Using this new formulation, the TMCMC algorithm is established in the context of network risk assessment.

3.2.1 Formulating Network Risk with Multivariate Normal Distribution

In this project, we focus on the special yet meaningful case of binary states for assets, namely, each asset has two states: a survival state that preserves its capacity and a failure state that reduces its capacity (e.g., due to detour or lane closure). To formulate TMCMC, the following transformation function $\tau: \mathbb{R} \to \{0,1\}$ is utilized:

$$\tau(\theta) = \begin{cases} 1 & if\ \theta < -\beta \\ 0 & otherwise \end{cases}$$

Equation 3.2 Transformation function for binary asset

where β = reliability index associated with the failure probability p such that $p \equiv \Pr[s = 1] = \Phi(-\beta)$, and Φ = CDF of a standard normal distribution; θ = a hidden standard normal random variable that can sample asset states using Equation 3.2. For n-dimensional space (a system with n binary assets), we can similarly leverage the transformation function $T: \mathbb{R}^n \to \{0,1\}^n$

$$T(\boldsymbol{\theta}) = \{\tau(\theta_i)\} \qquad where\ \boldsymbol{\theta} = \{\theta_i\}\ for\ i = 1,2,\dots,n$$

Equation 3.3 Transformation function for n binary assets

It is thus evident that the union of all $\boldsymbol{\theta} \in \mathbb{R}^n$, after transformation by $\boldsymbol{T}(\boldsymbol{\theta})$, corresponds to all system events $\mathcal{S}$ involving n binary assets (i.e., $\mathcal{S} = \{0,1\}^n$). In other word, for any system state

[1] Idiomatically, "black swan" events refer to events so rare that their occurrence cannot be anticipated. In contrast, the probability of occurrence for "grey swan" events, although very low, can still be estimated.

$\mathbf{s}_k \in \mathcal{S}$, we can find a domain $\Theta_k \subset \mathbb{R}^n$ such that all $\theta \in \Theta_k$ transform to $\mathbf{s}_k$. Now if $\boldsymbol{\theta}$ follows an independent multivariate normal distribution (with PDF represented by f_Θ), the risk associated with the system state $\mathbf{s}_k$ can be expressed as:

$$C(\boldsymbol{s}_k)p(\boldsymbol{s}_k) = C(\boldsymbol{s}_k) \cdot \int_{\Theta_k} f_\Theta(\boldsymbol{\theta})d\boldsymbol{\theta} = \int_{\Theta_k} C[T(\boldsymbol{\theta})]f_\Theta(\boldsymbol{\theta})d\boldsymbol{\theta}$$

Equation 3.4 Risk formulation given a specific system state $\mathbf{s}_k$

where $p(\mathbf{s}_k)$ and $C(\mathbf{s}_k)$ = probability of $\mathbf{s}_k$ and network-level consequence given $\boldsymbol{s}_k$, respectively; As a result, by considering all system states, the network risk can be expressed in terms of $\boldsymbol{\theta}$ as

$$\sum_{\boldsymbol{s}_k \in \mathcal{S}} C(\boldsymbol{s}_k)p(\boldsymbol{s}_k) = \int_\Theta C[T(\boldsymbol{\theta})]f_\Theta(\boldsymbol{\theta})d\boldsymbol{\theta}$$

Equation 3.5 Network risk formulation using multivariate normal distribution

Note that the derivation above assumes independent asset states for convenience. However, Equation 3.5 can be extended to correlated asset failures with Nataf transformation (Melchers & Beck 2018).

3.2.2 Estimating Network Risk with Transitional Markov Chain Monte Carlo (TMCMC)

The network risk formulated in Equation 3.5 has the same form as the "evidence" term in Bayes' theorem. Fundamentals of Bayes' theorem and terminologies relevant to the discussion of TMCMC algorithm are provided in Appendix C. This similarity inspires the adaptation of sampling methods for Bayesian updating to the context of network risk assessment. Specifically, the TMCMC algorithm stands out as it can efficiently estimate the "evidence" term in high dimensional space or with ill-posed posterior distributions (Ching & Chen 2007).

Figure 3.1 presents the flowchart of using the TMCMC-based method for network risk assessment. Conceptually, the TMCMC algorithm is effective for risk assessment because the samples generated in the process gradually transition from system states with high likelihood of occurrence (i.e., higher values of $f_\Theta(\boldsymbol{\theta})$) to systems states with high risks (i.e., states corresponding to larger products between the occurrence probabilities $f_\Theta(\boldsymbol{\theta})$ and the corresponding consequences $C[T(\boldsymbol{\theta})]$). Therefore, TMCMC provides a principled way to find system states critical to the network risk, allowing an accurate risk assessment with far less samples than crude MC simulation. Specifically, considering a total of $m + 1$ stages, the samples in stage j are drawn using MCMC from the following intermediate PDF:

$$f_j(\boldsymbol{\theta}) \propto \{C[T(\boldsymbol{\theta})]\}^{p_j} f_\Theta(\boldsymbol{\theta})$$
$$j = 0, \dots, m \quad and \quad 0 = p_0 < p_1 < \cdots < p_{m-1} < p_m = 1$$

Equation 3.6 Shape of intermediate PDF to generate samples from

As can be seen, initially with $p_0 = 0$, this is equivalent to sampling from the prior distribution $f_\Theta(\boldsymbol{\theta})$. As the tempering process continues, more and more samples with higher values of risk, i.e., $C[T(\boldsymbol{\theta})]f_\Theta(\boldsymbol{\theta})$, are generated. New samples are generated in two subsequent stages (e.g., from stage j to $j+1$) with the following two steps:

- Resample from the samples in the current stage following weights equal to $C[T(\boldsymbol{\theta})]^{p_{j+1}-p_j}$
- Use the selected samples as the heads of different Markov chains and generate samples in the new stage using MCMC.

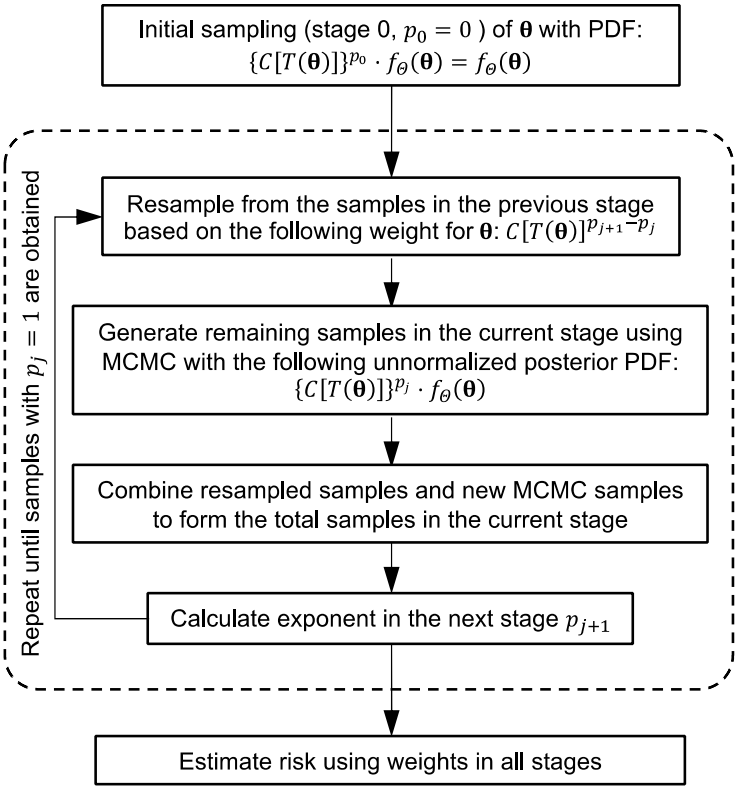

Figure 3.1 Flowchart of the TMCMC method

The samples in all stages can be utilized to estimate the "evidence", i.e., the network risk in this context, based on the following equation (Ching & Chen 2007):

$$\hat{R}_{net} = \prod_{j=0}^{m-1} \frac{\sum_{k=1}^{N_j} w\left(\boldsymbol{\theta}_k^{(j)}\right)}{N_j}$$

$$w\left(\boldsymbol{\theta}_k^{(j)}\right) = C\left[T\left(\boldsymbol{\theta}_k^{(j)}\right)\right]^{p_{j+1}-p_j}$$

Equation 3.7 Network risk estimated with the TMCMC method

where in each stage j, $\boldsymbol{\theta}_k^{(j)}$ = kth sample among all N_j samples. It should be noted that the samples of system states in the last stage of the aforementioned process may indicate different failure probabilities of assets compared to those associated with the reliability indices of assets. Based on

the formulation in Equation 3.5, these updated "failure probabilities" reflect the asset contribution to the network-level failure consequences, $C[T(\boldsymbol{\theta})]$. Therefore, besides estimating network risk, the samples in the last stage can be utilized to rank the contribution of different assets to the network risk, which can be insightful for risk-based asset ranking.

There are more details related to the implementation of TMCMC, e.g., the selection of proposal function in the MCMC step and the determination of tempering parameter in each stage p_j. These can be found in the original studies by Ching & Chen (2007) and followed up by Betz et al. (2016). In this project, the TMCMC algorithm described above is implemented based on the preliminary implementation in UQpy, a general-purpose Python toolbox for uncertainty quantification (Olivier et al. 2020). The original code in UQpy was improved and modified to enable parallel computing so that resources of high-performance computing can be fully capitalized.

3.3 ALGORITHM VERFICATION VIA NUMERICAL EXAMPLES

In this section, the effectiveness and efficiency of the TMCMC algorithm for network risk assessment are investigated based on a series of analytical examples. In practice, transportation networks often involve large quantities of assets, and it is difficult to anticipate whether "grey swan" events play a predominant role in the network risk. Therefore, the investigation is focused on the following two challenging cases for method verification: (a) high dimensional cases, i.e., systems with a large number of vulnerable assets (Case I); (b) risk assessment involving network effects and "grey swan" events (Case II). In both cases, the parameters in Table 3.1 are used as the parameters of TMCMC. The analytical examples are so designed that the precise network risk can be determined analytically and serves as the benchmark for verification.

Table 3.1 TMCMC parameters

Parameter	Value
Prior standard deviation	1.0
Resampling rate	10%
Number of samples per stage	5000
COV limit for stage progression	0.2
Number of chains during MCMC	10
Number of burn-in samples during MCMC	1000
Number of samples to skip during MCMC	10
Proposal standard deviation during MCMC	0.5

To demonstrate the advantage of the TMCMC algorithm over existing approaches, three methods for network risk assessment are compared, including:

- The TMCMC method: as described in Section 3.2;
- Crude MC method: system states are sampled based on $f_{\Theta}(\boldsymbol{\theta})$, and the average consequence associated with all sample states is the network risk;
- Risk-bound method: as described and implemented in Yang and Frangopol (2020).

To ensure fair comparison, the following ground rules are set up:

- The TMCMC method is implemented first for all examples; the number of consequence evaluations[1] and the total number of unique system states among all samples[2] are recorded;
- Crude MC simulation is carried out until the same number of consequence evaluations as that from the TMCMC implementation is reached;
- Risk-bound method is applied considering the same number of unique system states as that generated during the TMCMC implementation.

3.3.1 Case I: Effectiveness with Increasing Asset Numbers

For Case I, the analytical examples are designed using the following assumptions:

- Consider systems with increasing numbers of assets (5, 10, 30, and 50). For each system, the reliability index of an asset is randomly generated following a uniform distribution between 0 and 3. The assets are sorted from low to high reliability based on the reliability indices.
- The failure consequence of an asset (i.e., asset-level consequence) is assumed to be its rank in the sorted list of assets. For instance, the asset with the lowest reliability index (rank 1 in the sorted list) has a failure consequence of 1; the one with the highest has n_s (where n_s = number of assets).
- When multiple assets fail in the system, the consequence is the summation of asset-level consequences, i.e., the network effect is not present. Based on this simplification, the precise network risk used as the benchmark can be determined as follows:

$$\rho_I = \sum_{i=1}^{n_s} p_{f,i} \cdot C_i$$

Equation 3.8 Precise risk in Case I experiments

where $p_{f,i}$ and C_i = failure probability and asset-level consequence associated with asset i, respectively.

Following the ground rules outlined previously, Table 3.2 shows the results of risk estimation using different methods. The risk-bound method is accurate and efficient only when the system has a small number of assets (e.g., 5 and 10 assets in this example). In these cases, the risk-bound method considers all or most of the system states that can occur, resulting in accurate risk estimation. As the number of assets increases (e.g., starting with 30 assets), the risk-bound method significantly underestimates the network risk. By contrast, both TMCMC and MC can accurately estimate the network risk, though TMCMC yields results with more variability.

---

[1] In the analytical examples, the computation of consequences is fast and trivial. However, in practice, consequence evaluation refers to the computation of maximum flow capacity given the failure/survival states of all assets. This is usually the most computationally expensive step. A bookkeeping database is usually maintained so if the system states are the same, the maximum flow capacity is retrieved from the database instead of being computed again.

[2] The samples used to count unique system states include (a) samples generated in each stage of the transition process and (b) the discarded samples in the burn-in and skip phases of MCMC.

Table 3.2 Results of method comparison (statistics of the estimated risks are determined with 5 runs with different random seeds)

(a) 5 assets (precise risk = 2.205)

Method	Average risk	Standard deviation	Max	Min
TMCMC	2.188	0.024	2.222	2.161
MC	2.186	0.002	2.188	2.185
Bound	2.205	0.000	2.205	2.205

(b) 10 assets (precise risk = 7.527)

Method	Average risk	Standard deviation	Max	Min
TMCMC	7.534	0.080	7.612	7.420
MC	7.471	0.007	7.478	7.462
Bound	7.519	0.001	7.521	7.517

(c) 30 assets (precise risk = 39.45)

Method	Average risk	Standard deviation	Max	Min
TMCMC	39.40	0.30	39.91	39.15
MC	39.41	0.02	39.44	39.38
Bound	10.84	0.42	11.42	10.28

(d) 50 assets (precise risk = 91.41)

Method	Average risk	Standard deviation	Max	Min
TMCMC	90.70	0.95	92.12	89.75
MC	91.71	0.07	91.79	91.62
Bound	2.60	0.00	2.60	2.60

3.3.2 Case II: Effectiveness in Risk Assessment involving Network Effects And "Grey Swan" Events

Case I indicates that both TMCMC and MC can be effective in assessing risks from large numbers of assets. For Case II, a separate set of numerical experiments is constructed to further differentiate the effectiveness of TMCMC and MC. Herein, two issues in realistic problems of network risk assessment are addressed:

(a) The existence of network effects, i.e., the failure consequence of multiple asset failures may be larger than the summation of the consequences of individual failures;
(b) As a result, network risk may be dominate by "grey swan" events (low-probability events with high consequences) involving multiple asset failures.

To this end, numerical experiments are designed as follows:

- We consider a system consisting of 30 assets. Similar to Case I, reliability indices are randomly generated (uniformly between 0 and 3) and assigned to each asset.
- To model "grey swan" events, only five assets with the highest reliability are considered to induce adverse consequences. The consequence of each individual failure is assumed to follow the equation below:

$$C_i = 10^{\frac{(i-1)\beta_i}{n_s-1}}$$

Equation 3.9 Consequence of individual asset failure in Case II experiments

where β_i = reliability index, i is the rank in the ordered asset list ($i = 26, 27, \dots, 30$ for the top five most reliable assets), and $n_s = 30$ is the total number of assets.

- To model the network effect, the following two assumptions are adopted: (a) no matter how many assets fail, the network consequence only appears if at least one of the top five most reliable assets fails; (b) when more than one of the top five assets fail, the network consequence is the product of individual failure consequences determined by Equation 3.9.

Since only 5 out of the 30 assets are relevant to network risk, the precise value of network risk can be determined by parsing through all ($2^5-1=$) 31 system states that have adverse effects. On the other hand, TMCMC and MC methods are implemented respectively to estimate the network risk involving all 30 assets. Each method is implemented for 10 times to derive statistics. Figure 3.2 shows the estimated network risks using both methods, presented in the form of a box-whisker plot. Again, TMCMC can accurately estimate the network risk in Case II experiments. The percentage error of the estimated risk ranges from -11.31% to +7.18% compared to the precise value (45.001), with the mean of the 10 implementations closely matching the precise value (44.659 vs 45.001). In contrast, most of the 10 MC implementations yield severely underestimated risk due to the lack of representation of "grey swan" events among the samples. Occasionally, the "grey swan" events may be overrepresented, yielding drastically overestimated risk. In summary, the MC method fails to reliably estimate risk due to the difficulty in sampling "grey swan" events.

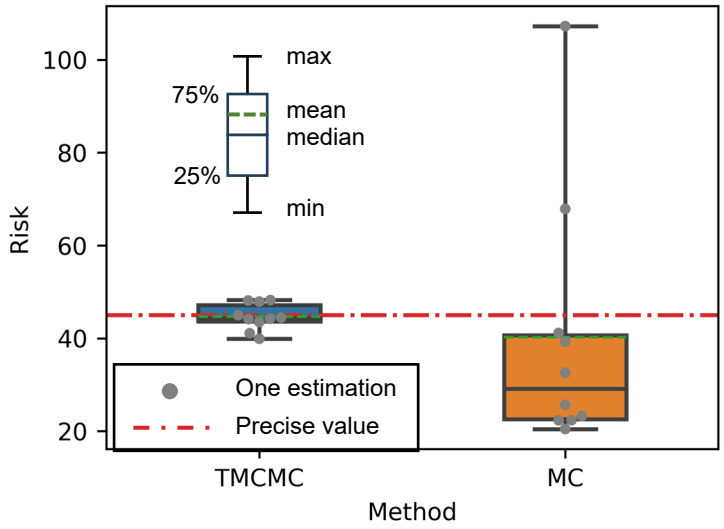

Figure 3.2 Comparison of results in Case II experiments (considering network effects and grey swan events)[1]

3.4 CASE STUDY WITH OREGON HIGHWAY NETWORK

In this section, a transportation network of a realistic scale is analyzed using the TMCMC method. The case study is focused on the entire Oregon highway network with thousands of vulnerability bridges. The reliability indices of each link with vulnerable bridges are randomly assigned similar to what is performed in Section 3.3. Due to this random assignment of link reliability, the results of this case study are only used for algorithmic validation and should not be regarded as the true risk related to the Oregon highway network. The goal herein is to validate the effectiveness of the TMCMC method for realistic large-scale networks.

[1] In the box-whisker plot, the box encloses data from the 25th to the 75th percentiles, and the whiskers are minimum and maximum values among the data. The solid and the dash lines between the whiskers are median and mean values, respectively.

3.4.1 Developing Network Model for Oregon Highway System

The geospatial data related to the Oregon highway network are extracted from OpenStreetMap[1] database (Contributors 2022). To focus on highway networks, only road segments labeled as "motorway", "trunk", and "primary" are extracted (Contributors 2022). This filter allows us to cover the majority of key highway bridges managed by Oregon Department of Transportation (ODOT). The raw geospatial data are converted to a directed graph model using OSMnx, a Python-based tool to extract, model, analyze, and visualize street networks and other geospatial features from OpenStreetMap[15] (Boeing 2017). Details related to the data extract and model creation are provided in Appendix D.

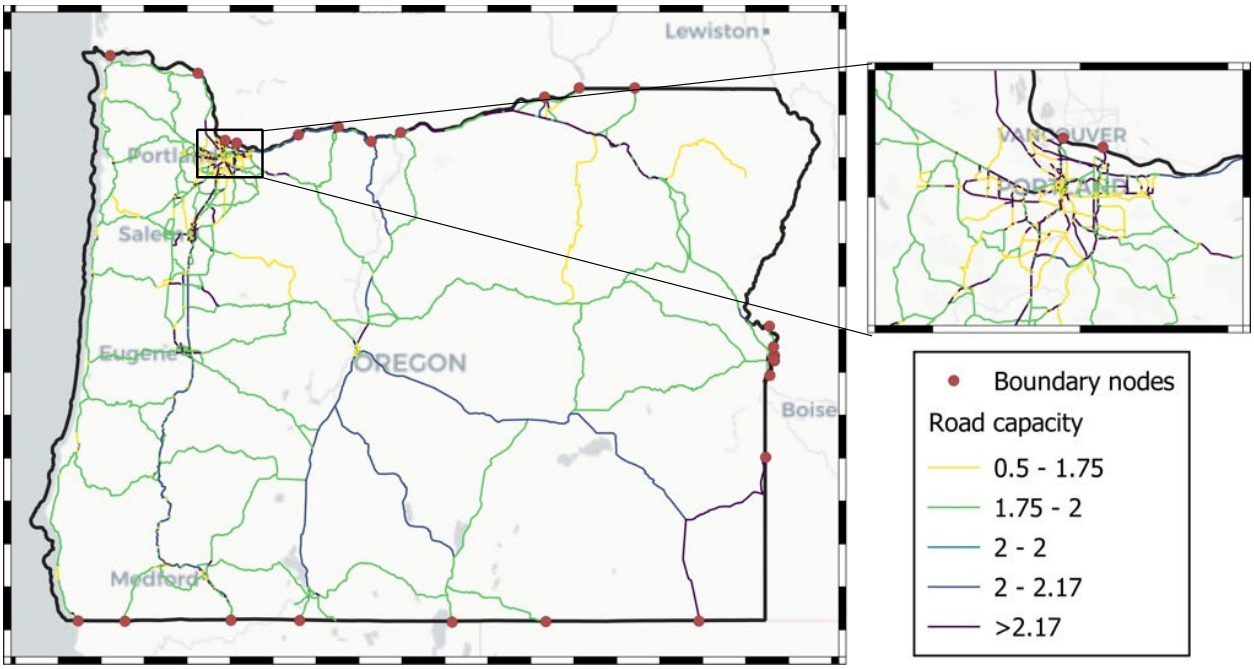

Figure 3.3 Oregon highway network model (from OpenStreetMap[15])

Figure 3.3 shows the highway network under consideration. Boundary nodes representing the nodes into and out of the State of Oregon are also highlighted in Figure 3.3. OD pairs are selected[2] from these boundary nodes to estimate the maximum flow capacity through the highway network (referred to hereafter as the throughput). The nominal flow capacity of a link is computed using the following equation:

$$f_i = n_{lane} \cdot \frac{v_{lane}}{v_{nom}}$$

Equation 3.10 Nominal link capacity

[1] The U.S. Government does not endorse products or manufacturers. They are included for informational purposes only and are not intended to reflect a preference, approval, or endorsement of any one product or entity.

[2] Any two boundary nodes more than 50 miles apart are assumed to be a valid OD pair for the determination of network throughput.

where f_i = capacity of link i; n_{lane} = number of lanes; v_{lane} = speed limit (mph); v_{nom} = nominal speed on a highway, assumed to be 60 mph in this study. Both the lane numbers and the speed limits are available from OpenStreetMap for all links. If a link contains multiple lane numbers and speed limits, the minimum lane number and the average speed limit are substituted into Equation 3.10 to compute the link capacity.

The graph in Figure 3.3 contains 6,437 nodes and 10,637 links. Among the links, 1,938 links carry bridges (referred to hereafter as bridge links) that may fail due to either deterioration or extreme events. Similar to the previous numerical examples, the reliability index of each bridge link is randomly assigned by uniformly sampling between 0 and 3. In practice, three steps can be implemented to estimate these reliability indices:

(a) Locate all bridges on a link: this can be achieved with geo-processing tools[1] widely available in common GIS platforms (e.g., QGIS[2]).
(b) Conduct structural reliability or fragility analysis to compute the reliability indices of all bridges on the link
(c) Carry out system reliability analysis for a series system (Ditlevsen & Madsen 2005; Der Kiureghian 2022) to determine link reliability.

If a bridge link fails, it is assumed that all traffic on the link will be diverted to a local detour near the link, modeled by reducing the link capacity to (1 lane × 20 mph / 60 mph =) 0.333. This reduction decreases the throughput of the network. This decrease in throughput, normalized by the throughput of the intact network, is used to assess the indirect risk of bridge failures. Decreases in throughput exhibit the network effect since the consequence from multiple link failures is generally different from the summation of consequences from individual link failures.

To achieve efficient computation of network throughput, the highway network in Figure 3.3 is converted to a computational graph containing only information needed for the throughput calculation. Figure 3.4 shows the computational graph generated with NetworkX[18], a Python package for creating and analyzing complex networks (Hagberg et al. 2008). Note that this graph only preserves (a) the connections between different nodes and (b) link capacities needed for the flow calculation. It does not contain geospatial properties of nodes and links. Instead, the graph is presented in Figure 3.4 using spectral layout.

[1] For instance, a step-by-step implementation within QGIS can be found via this link: https://gis.stackexchange.com/questions/381056/find-nearest-line-feature-from-point-in-qgis

[2] The U.S. Government does not endorse products or manufacturers. They are included for informational purposes only and are not intended to reflect a preference, approval, or endorsement of any one product or entity.

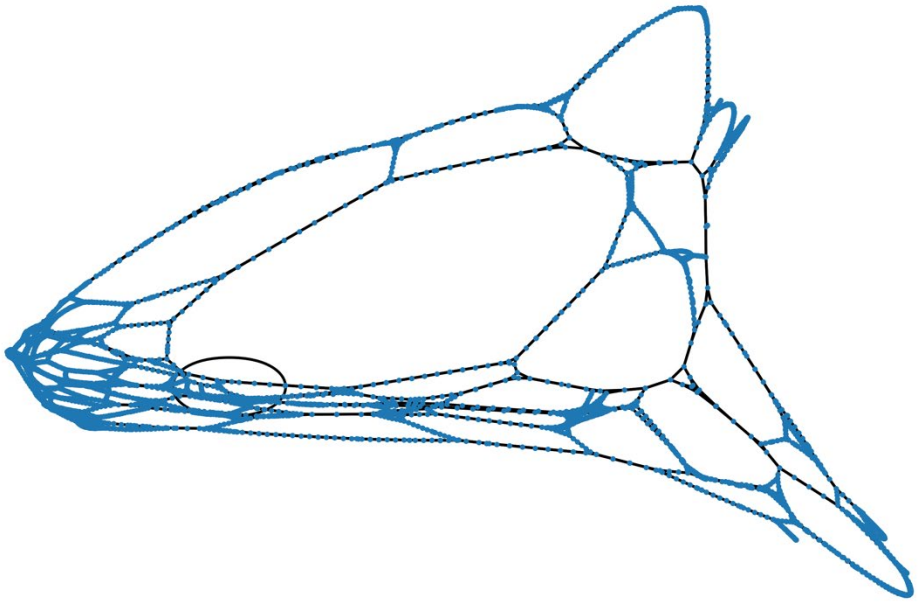

Figure 3.4 Computational graph of Oregon highway network

3.4.2 Mobility Risk Assessment of Oregon Highway Network

Given the network effect, indirect risk assessment for all bridge links constitutes a high dimensional problem involving 1,938 binary variables. At this scale, the risk bound method no longer works based on the results from previous numerical examples. It is also not clear whether there are "grey swan" events dominating the network risk. Therefore, network risk assessment is carried out using the TMCMC method. Table 3.3 summarizes the TMCMC parameters used for the network risk assessment.

Table 3.3 TMCMC parameters for Oregon highway network

Parameter	Value
Prior standard deviation	1.0
Resampling rate	10%
Number of samples per stage	8000
COV limit for stage evolution	0.2
Number of chains during MCMC	80
Number of burn-in samples during MCMC	1000
Number of samples to skip during MCMC	10
Proposal standard deviation during MCMC	0.5

Using the TMCMC method, the mobility risk of this network is estimated at 0.3360. This indicates that given the failure probabilities of all 1,938 bridge links, the expected decrease in flow capacity is 33.60%. The computation is carried out on a stack server using 80 processes and has a wall-clock runtime of 22.66 hours. In total, 44,213 unique system states are analyzed. The result herein demonstrates the effectiveness of the TMCMC method in a realistic risk assessment setting.

In addition to risk estimation, a useful byproduct of the TMCMC method is the samples generated in the last stage. Based on the derivation of TMCMC, system states frequently appearing in the

last stage of sampling represent failure patterns that have large contributions to the network risk. Figure 3.5 presents the failure patterns associated with the top three most frequent samples in the last stage of TMCMC sampling. These identified assets provide valuable insights into intervention priorities that can have the most significant benefit in reducing risk. It should be noted that the results in Figure 3.5 hinges on various assumptions adopted in the case study. For instance, the reliability indices of bridges are randomly assigned instead of derived from asset conditions or fragilities. In collaboration with ODOT engineers, a calibrated case study with realistic input will be pursued in the second phase of the project.

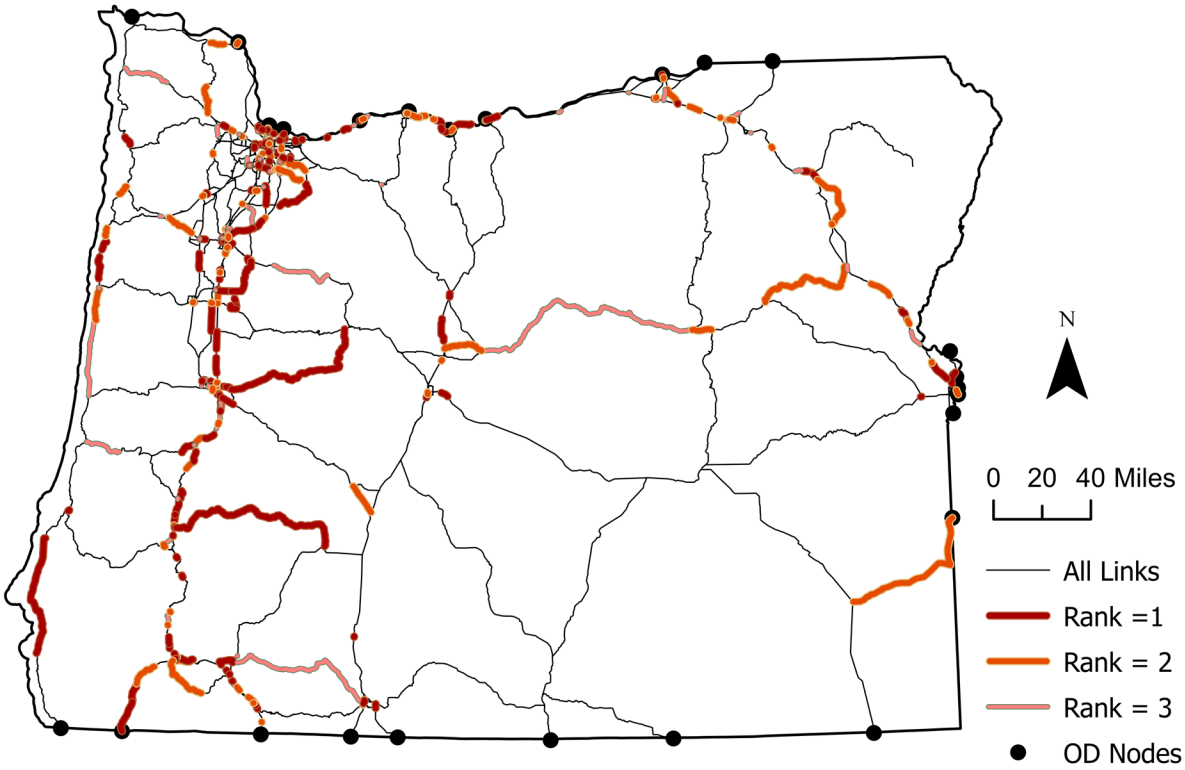

Figure 3.5 High risk bridge links (ranks represent the 1st, 2nd, and 3rd most frequent samples in the last stage of TMCMC sampling)

3.5 SUMMARY

Chapter 3 introduces an effective and efficient method to assess indirect risk of transportation systems when the network performance indicator exhibits considerable network effects. The effectiveness of the mobility risk assessment method is demonstrated through a number of analytical examples and a real-world case study on the Oregon highway network.

Compared to existing methods, the advantages of the new TMCMC method becomes ever more salient when (a) hundreds to thousands of assets are involved, (b) indirect consequences exhibit considerable network effects, and/or (c) the network risk is dominated by a small number of low probability, high consequence events. In addition to assessing risk, TMCMC is also capable of identifying routes and assets that contribute the most to the network risk, thereby offering insights to intervention planning.

Although the formulation and case study are primarily focused on network throughput, the network performance indicator can be adapted to other measures that may be relevant to the decision-making. For instance, if the link capacities are set to one for intact links and zero for failed links, the maximum flow capacity analyzed herein directly reduces to the connectivity between OD pairs. This adaptation can be useful when the risk is assessed in terms of the community's accessibility to critical public services after a disaster event.

CHAPTER 4

CONCLUSIONS AND NEXT STEPS

Practical frameworks and methods for risk-based bridge and tunnel management are presented in this report. The research presented herein is focused on the consistent and objective risk assessment of critical transportation assets. Both direct and indirect consequences are considered. For direct risk assessment, the emphasis is on the integration of structural deterioration and extreme event risk as well as the implementation in and implications to transportation asset management. For indirect risk assessment, the focus is on the development of an effective method to consider system-level user risks (e.g., network throughput) that rely on the network topology of interconnected assets.

The following conclusions can be drawn from Phase I study:

- (Chapter 1) Risks from structural deterioration and extreme events can be integrated to obtain lifetime risks expressed in monetary units. This integration allows for risk-based bridge and tunnel management to better coordinate between condition preservation and risk mitigation activities. To realize these benefits, it is important to provide objective risk estimates that are consistent across different hazards, analysis tools, and transportation agencies.
- (Chapter 2) To achieve objective risk assessment, a novel approach based on weighted hazard scenarios is established to fill the gap between risk analysis and asset management. Rather than rely on expert elicitation to identify hazard scenarios, the new approach can generate scenarios weighted by hazard intensities and frequencies, structural fragilities, and damage consequences. This enables accurate risk assessment that can be consistently applied to different hazards and limits biases from the agency or its analysts. Compared to existing risk assessment methods in transportation asset management systems, the new approach can yield much higher accuracy with the same number of hazard scenarios.
- (Chapter 2) The new approach for objective risk assessment is also applicable to analyses involving interacting hazards such as the analysis of seismic risk compounded by structural deterioration. For stationary hazards (i.e., hazard frequency and intensity do not change over time), it is found that as long as the deterioration effect is reflected in the expected consequences for different hazard scenarios, the same set of hazard scenarios can be used over the entire service life of the structure without introducing noticeable errors. It is also demonstrated that inaccurate risk assessment may obscure the benefit-to-cost ratios of different maintenance strategies that have different effects on deterioration. Therefore, the approach enables risk-based transportation asset management.
- (Chapter 3) An effective and efficient method is developed to assess the indirect risk of large-scale transportation asset networks. The advantage of the new method is especially salient when (a) the performance indicator exhibits network effects, i.e., when the system-level failure consequences is more severe than the sum of consequences of individual failures, and (b) when the network risk is dominated by low probability, high consequence events. The new method can handle regional transportation networks of realistic scales (e.g., hundreds to thousands of assets). In addition to assessing risk, the method is also capable of identifying routes and assets that contribute the most to the network risk, thereby offering insights to intervention planning.

Built upon the results from Phase I study, the following steps may be taken for Phase II and future studies:

- Phase II study should focus on the further validation of case study results presented in Chapter 3. There are several fictitious assumptions adopted in the case study to illustrate the real-world capability of the new approach to assess indirect risk. Phase II will examine and improve these assumptions such as the proper consideration of condition ratings when assigning asset failure probabilities. The identified links crucial to the system performance will be compared with the critical links established empirically by the transportation agencies. Overlapping and differences should be investigated.
- The risk integral hinges on several models that deserve further investigation, including (a) the probabilities of service disruption for deteriorated assets in different condition states and (b) the time- or condition-based fragility curves that consider the effect of deterioration on structural vulnerability under extreme events.
- For the illustration of the risk-based asset management framework and methodology, seismic hazards have been heavily relied upon due to their relative maturity in terms of hazard characterization and structural fragility models. Although this project points to a principled approach to other hazards, application to non-seismic hazards and the associated knowledge/data gaps should be further investigated.
- For indirect risk assessment, this study focuses primarily on network throughput. However, the approach to network risk assessment should also be adaptable to other system-level performance measures that may be relevant to different decision-making scenarios. For instance, the connectivity between origin-destination pairs can be useful when hazard risk is assessed in terms of communities' accessibility to critical public services after a disaster event.

ACKNOWLEDGMENTS

The authors would like to acknowledge the support from Federal Highway Administration, especially from the technical point of contact of the project, Jia-Dzwan (Jerry) Shen. The help and valuable comments received from the members of the technical panel are also greatly appreciated. Panel members include Bert H. Hartman (ODOT), Albert Nako (ODOT), Derek Constable (FHWA), Derek Soden (FHWA), Elizabeth Habic (FHWA), Jeffrey Ger (FHWA), Kornel Kerenyi (FHWA), Robert Kafalenos (FHWA).

REFERENCES

AASHTO, 2021. AASHTOWare Bridge Management. Available at: https://www.aashtowarebridge.com.

Abramowitz, M. & Stegun, I., 1972. *Handbook of Mathematical Functions with Formulas, Graphs, and Mathematical Table* , 10th ed., Washington, DC: National Bureau of Standards (NBS).

Ahuja, R.K., Magnanti, T.L. & Orlin, J.B., 1993. *Network Flows: Theory, Algorithms, and Applications*, Upper Saddle River, NJ: Prentice Hall.

Baker, J., Bradley, B. & Stafford, P., 2021. *Seismic Hazard and Risk Analysis*, Cambridge, UK: Cambridge University Press.

Baker, J.W., 2013. Introduction to Probabilistic Seismic Hazard Analysis. *White Paper Version 2.0.1*. Available at: http://dx.doi.org/10.1016/j.strusafe.2008.06.002.

Basöz, N. & Mander, J.B., 1999. *Enhancement of the Highway Transportation Lifeline Module in HAZUS*, National Institute of Building Sciences.

Bektas, B.A. & Albughdadi, A.J.M., 2020. Drivers of Bridge Decommissioning in the United States. *Transportation Research Record: Journal of the Transportation Research Board*, 2674(8): 591–603. Available at: http://journals.sagepub.com/doi/10.1177/0361198118822810.

Bell, M.G.H. & Iida, Y., 1997. *Transportation Network Analysis*, Chichester, England: Wiley.

Bensi, M., Kiureghian, A. Der & Straub, D., 2015. Framework for post-earthquake risk assessment and decision making for infrastructure systems. *ASCE-ASME Journal of Risk and Uncertainty in Engineering Systems, Part A: Civil Engineering*, 1(1): 04014003. Available at: http://ascelibrary.org/doi/10.1061/AJRUA6.0000810.

Betz, W., Papaioannou, I. & Straub, D., 2016. Transitional Markov Chain Monte Carlo: Observations and Improvements. *Journal of Engineering Mechanics*, 142(5):.

Bhandari, A., 2023. *Uncertainty Quantification and Fragility Development of Deteriorating RC Bridge Piers*. MS Thesis. Portland, OR: Portland State University.

Bocchini, P. & Frangopol, D.M., 2011. Generalized bridge network performance analysis with correlation and time-variant reliability. *Structural Safety*, 33(2): 155–164. Available at: http://dx.doi.org/10.1016/j.strusafe.2011.02.002.

Boeing, G., 2017. OSMnx: New methods for acquiring, constructing, analyzing, and visualizing complex street networks. *Computers, Environment and Urban Systems*, 65: 126–139. Available at: https://linkinghub.elsevier.com/retrieve/pii/S0198971516303970.

Buckle, I., Friedland, I., Mander, J., Martin, G., Nutt, R. & Power, M., 2006. *Seismic Retrofitting Manual for Highway Structures: Part 1 - Bridges*, McLean, VA: Office of Infrastructure Research and Development, Federal Highway Administration (FHWA).

Chang, L., Peng, F., Ouyang, Y., Elnashai, A.S. & Spencer, B.F., 2012. Bridge seismic retrofit program planning to maximize postearthquake transportation network capacity. *Journal of Infrastructure Systems, ASCE*, 18(2): 75–88. Available at: http://ascelibrary.org/doi/abs/10.1061/(ASCE)IS.1943-555X.0000138.

Chapra, S.C. & Canale, R.P., 2021. *Numerical Methods for Engineers* , 8th ed., New York, NY: McGraw-Hill.

Ching, J. & Chen, Y.-C., 2007. Transitional Markov Chain Monte Carlo Method for Bayesian Model Updating, Model Class Selection, and Model Averaging. *Journal of Engineering Mechanics*, 133(7): 816–832. Available at: https://ascelibrary.org/doi/10.1061/%28ASCE%290733-9399%282007%29133%3A7%28816%29.

Contributors, 2022. OpenStreetMap Wiki. Available at: https://wiki.openstreetmap.org/wiki/Main_Page [Accessed August 21, 2023].

Cornell, C.A., Banon, H. & Shakal, A.F., 1979. Seismic motion and response prediction alternatives. *Earthquake Engineering & Structural Dynamics*, 7(4): 295–315.

Der Kiureghian, A., 2022. *Structural and System Reliability*, Cambridge, UK: Cambridge University Press.

Ditlevsen, O. & Madsen, H.O., 2005. *Structural Reliability Methods*, Chichester, England: Wiley.

FEMA, 2009. *Hazus-MH Flood Model Technical Manual*, Washington, DC: Federal Emergency Management Agency (FEMA).

FEMA, 2023. HAZUS. Available at: https://www.fema.gov/flood-maps/products-tools/hazus [Accessed November 1, 2023].

Ghosn, M., Dueñas-Osorio, L., Frangopol, D.M., McAllister, T., Bocchini, P., Manuel, L., Ellingwood, B.R., Arangio, S., Bontempi, F., Shah, M., Akiyama, M., Biondini, F., Hernandez, S. & Tsiatas, G., 2016. Performance indicators for structural systems and infrastructure networks. *Journal of Structural Engineering, ASCE*, 142(9): 1–18.

Hagberg, A., Swart, P. & S Chult, D., 2008. Exploring network structure, dynamics, and function using networkx. In *Proceedings of the 7th Python in Science Conference (SciPy2008)*. Pasadena, CA: SciPy Organizers, 1–5. Available at: https://www.osti.gov/biblio/960616.

Inkoom, S., Sobanjo, J.O., Thompson, P.D., Kerr, R. & Twumasi-Boakye, R., 2017. Bridge Health Index: Study of Element Condition States and Importance Weights. *Transportation Research Record: Journal of the Transportation Research Board*, 2612(1): 67–75. Available at: http://journals.sagepub.com/doi/10.3141/2612-08.

McGuire, R.K., 2004. *Seismic Hazard and Risk Analysis*, Oakland, CA: Earthquake Engineering Research Institute (EERI).

Melchers, R.E. & Beck, A.T., 2018. *Structural Reliability Analysis and Prediction* , 3rd ed., Hoboken, NJ: John Wiley & Sons Ltd.

Morlok, E.K. & Chang, D.J., 2004. Measuring capacity flexibility of a transportation system. *Transportation Research Part A: Policy and Practice*, 38(6): 405–420.

Muntasir Billah, A.H.M. & Shahria Alam, M., 2015. Seismic fragility assessment of highway bridges: a state-of-the-art review. *Structure and Infrastructure Engineering*, 11(6): 804–832. Available at: http://www.tandfonline.com/doi/abs/10.1080/15732479.2014.912243.

Newman, M., 2018. *Networks* , 2nd ed., Oxford, UK: Oxford University Press.

NIST, 2023. Interdependent Networked Community Resilience Modeling Environment (IN-CORE). Available at: https://incore.ncsa.illinois.edu [Accessed November 1, 2023].

Olivier, A., Giovanis, D.G., Aakash, B.S., Chauhan, M., Vandanapu, L. & Shields, M.D., 2020. UQpy: A general purpose Python package and development environment for uncertainty quantification. *Journal of Computational Science*, 47: 101204.

Patriksson, M., 2015. *The Traffic Assignment Problem: Models and Methods*, Mineola, NY: Dover Publications.

Rokneddin, K., Ghosh, J., Dueñas-Osorio, L. & Padgett, J.E., 2014. Seismic reliability assessment of aging highway bridge networks with field instrumentation data and correlated failures, II: Application. *Earthquake Spectra*, 30(2): 819–843.

Saydam, D., Bocchini, P. & Frangopol, D.M., 2013. Time-dependent risk associated with deterioration of highway bridge networks. *Engineering Structures*, 54: 221–233. Available at: http://dx.doi.org/10.1016/j.engstruct.2013.04.009.

Vishnu, N., Kameshwar, S. & Padgett, J.E., 2023. Road transportation network hazard sustainability and resilience: correlations and comparisons. *Structure and Infrastructure Engineering*, 19(3): 345–365. Available at: https://www.tandfonline.com/doi/full/10.1080/15732479.2021.1945114.

Weisstein, E.W., 1995. *Wolfram MathWorld: The Web's Most Extensive Mathematics Resource*, Champaign, IL: Wolfram Research.

Western, J., Bye, P., Valeo, M., Thompson, P.D. & Frazier, E., 2016. *NCHRP 20-07/Task 378 Final Report: Assessing Risk for Bridge Management*, Washington, DC: National Cooperative Highway Research Program (NCHRP).

Yang, D.Y., 2022. Deep Reinforcement Learning–Enabled Bridge Management Considering Asset and Network Risks. *Journal of Infrastructure Systems*, 28(3): 04022023. Available at: https://ascelibrary.org/doi/10.1061/%28ASCE%29IS.1943-555X.0000704.

Yang, D.Y. & Frangopol, D.M., 2018. Risk-informed bridge ranking at project and network levels. *Journal of Infrastructure Systems*, 24(3): 04018018. Available at: http://ascelibrary.org/doi/10.1061/%28ASCE%29IS.1943-555X.0000430.

Yang, D.Y. & Frangopol, D.M., 2019. Societal risk assessment of transportation networks under uncertainties due to climate change and population growth. *Structural Safety*, 78: 33–47. Available at: https://linkinghub.elsevier.com/retrieve/pii/S0167473018301346.

Yang, D.Y. & Frangopol, D.M., 2020. Life-cycle management of deteriorating bridge networks with network-level risk bounds and system reliability analysis. *Structural Safety*, 83: 101911. Available at: https://doi.org/10.1016/j.strusafe.2019.101911.

APPENDIX A GAUSSIAN QUADRATURE FOR NUMERICAL INTEGRATION

An n-point Gaussian quadrature is a rule to carry out integration numerically using integrand values at n strategically selected locations (termed integration points) and their associated weights (Chapra & Canale 2021). The most common Gaussian quadrature is the Gauss-Legendre quadrature, which is given as follows for a one-dimensional (1D) integral over domain $[-1, 1]$ (Abramowitz & Stegun 1972):

$$\int_{-1}^{1} f(\xi)\, d\xi \approx \sum_{i=1}^{n} \eta_i f(\xi_i)$$

Equation A.1 Gauss-Legendre quadrature

where $f(\xi)$ = integrand function; ξ_i $(i = 1,2, \dots, n)$ = n integration points within $[-1, 1]$; η_i = the associated weights. It is worth mentioning that the quadrature rule is exact if $f(\xi)$ is a polynomial of up to $2n - 1$ degrees (Weisstein 1995). Therefore, if $f(\xi)$ can be reasonably approximated by a polynomial of up to $2n - 1$ degrees, the error of this quadrature can be small. Also, the domain $[-1,1]$ can be easily converted to any definite integral domain through transformation (Abramowitz & Stegun 1972). When singularities arise at the endpoints of the integral domain or when semi-infinite or infinite intervals are involved, other Gaussian quadrature rules can be applied, such as Chebyshev-Gauss or Gauss-Hermite quadrature (Weisstein 1995).

Given the number of integration points n, the integration points ξ_i and weights η_i are independent of the integrand function and can be found in several references (e.g., Weisstein 1995). Table A.1 shows the integration points and weights for $n = 2$ to $n = 6$ However, given an acceptable level of the approximation error, the form of $f(\xi)$ can affect the number of integration points needed. Specifically, if a function can be well approximated by a lower order polynomial, the required number of integration points is small, and vice versa.

Table A.1 Integration points and weights for Gauss-Legendre quadrature

Number of integration points n	Integration point ξ_i	Weight η_i
$n = 2$	–0.5774, 0.5774	1
$n = 3$	–0.7746, 0, 0.7746	0.5556, 0.8889, 0.5556
$n = 4$	–0.8611, –0.3340, 0.3340, 0.8611	0.3479, 0.6521, 0.6521, 0.3479
$n = 5$	–0.9062, –0.5385, 0, 0.5385, 0.9062	0.2369, 0.4786, 0.5689, 0.4786, 0.2369
$n = 6$	–0.9325, –0.6612, –0.2386, 0.2386, 0.6612, 0.9325	0.1713, 0.3608, 0.4679, 0.4679, 0.3608, 0.1713

APPENDIX B NETWORK MODELING WITH GRAPHS

To determine flow capacity and many other transportation performance indicators, a transportation system needs to be converted to a network model, also known as a graph (Newman 2018). A graph consists of vertices (also known as nodes) and edges (also known as links). Both vertices and edges can be used to represent transportation assets (e.g., a bridge, tunnel, or pavement segment)

depending on their spatial scales. In network sciences, all graphs can be categorized as follows (Newman 2018):

- Undirected simple graph: Any two nodes can only be connected by at most one link (hence the name "simple"). All links are undirected, i.e., they can carry bidirectional traffic.
- Directed simple graph: These graphs are also simple graphs. However, the links have directions, i.e., a link connecting from node i to node j is different from a link connecting from node j to node i.
- Undirected multigraph: These graphs have undirected links. However, two nodes can be connected by more than one link.
- Directed multigraph: These graphs are multigraphs with directed links.

In the most general case, transportation networks are modeled as directed multigraphs. However, finding the maximum flow between an OD pair is challenging in this case due to the ambiguities of flow distribution among different links connecting two nodes (Newman 2018). Therefore, a directed multigraph obtained using OSMnx[1] is converted to a directed simple graph by keeping only the shortest link among all links connecting two nodes (Boeing 2017). For major highway networks without one-way roads, it is also possible to convert directed simple graphs to undirected simple graphs to further enhance the computational efficiency.

Using a directed simple graph, the maximum flow from the origin node s to the destination node t can be formulated as the following optimization problem (Ahuja et al. 1993):

$$max\ v_{st}$$

$$subject\ to$$

$$\sum_{v:(s,v)\in\mathcal{E}} f_{sv} - \sum_{u:(u,s)\in\mathcal{E}} f_{us} = v_{st}$$

$$\sum_{v:(t,v)\in\mathcal{E}} f_{tv} - \sum_{u:(u,t)\in\mathcal{E}} f_{ut} = -v_{st}$$

$$0 \le f_{uv} \le c_{uv} \quad \forall (u,v) \in \mathcal{E}$$

$$\sum_{u:(u,v)\in\mathcal{E}} f_{uv} = \sum_{u:(v,u)\in\mathcal{E}} f_{vu} \quad \forall v \in \mathcal{V} \setminus \{s,t\}$$

Equation B.1 Formulation of maximum flow in a graph

[1] The U.S. Government does not endorse products or manufacturers. They are included for informational purposes only and are not intended to reflect a preference, approval, or endorsement of any one product or entity.

where v_{st} = the flow from s to t; f_{ij} = flow on link (i,j) connecting from vertex i to vertex j if (i,j) exists in the set of all edges $\mathcal{E}$; c_{uv} = capacity of link (u,v), which is related to the number of lanes and the speed limit on the link; $\mathcal{V}$ and $\mathcal{V} \setminus \{s,t\}$ = set of all vertices and set of all vertices except for s and t, respectively. The first and second constraints in the formulation above represent that the total flow originating from node s equal the total flow sinking into vertex t. The third constraint is the capacity constraint, i.e., the flow on an edge cannot exceed its capacity. The last constraint models the conservation of flows, i.e., the total flow into a vertex should equal that out of the same vertex. The maximum flow capacity between OD pairs within a network is an important performance indicator of transportation networks and other infrastructure systems with interconnected assets.

APPENDIX C BAYESIAN UPDATING WITH TRANSITIONAL MARKOV CHAIN MONTE CARLO

Based on Bayes' theorem, the posterior PDF of system parameters conditioned on the observations of the system output can be expressed as

$$f(\boldsymbol{\theta}|D) = \frac{f(D|\boldsymbol{\theta}) \cdot f(\boldsymbol{\theta})}{\int_{\boldsymbol{\theta}} f(D|\boldsymbol{\theta}) \cdot f(\boldsymbol{\theta}) d\boldsymbol{\theta}}$$

Equation C.1 Bayesian theorem

where $f(\boldsymbol{\theta})$ = prior PDF of system parameters $\boldsymbol{\theta}$; $f(D|\boldsymbol{\theta})$ = likelihood associated with system observation D, i.e., the conditional PDF of D given the system parameters $\boldsymbol{\theta}$. The numerator $f(D|\boldsymbol{\theta}) \cdot f(\boldsymbol{\theta})$ describe the shape of the posterior PDF. The denominator $\int_{\boldsymbol{\theta}} f(D|\boldsymbol{\theta}) \cdot f(\boldsymbol{\theta}) \mathrm{d}\boldsymbol{\theta}$ serves as a normalization constant so that $f(\boldsymbol{\theta}|D)$ satisfies the requirement of a PDF, i.e., the volume under the function is equal to 1. In the context of Bayesian updating, this normalization constant is also called the "evidence". Sampling from posterior PDF $f(\boldsymbol{\theta}|D)$ is challenging because of the following reasons:

- The posterior PDF does not always follow an analytical distribution;
- The evidence is only known by a factor, i.e., only the value of $f(D|\boldsymbol{\theta}) \cdot f(\boldsymbol{\theta})$ is known.

Most Markov Chain Monte Carlo (MCMC) methods focus on solving the first challenge by directly sampling from a posterior distribution without knowing the evidence. Transitional Markov Chain Monte Carlo (TMCMC), first proposed by Ching & Chen (2007) and later refined by Betz et al. (2016), is an efficient method that can both generate posterior samples and estimate the evidence. It is the ability to estimate evidence that directly contributes to the accurate assessment of network risk.

The connection between the evidence (i.e., denominator in Equation C.1) and the network risk formulated in Equation 3.5 is shown by equating the likelihood function $f(D|\boldsymbol{\theta})$ with $C[T(\boldsymbol{\theta})]$ in Equation 3.5. In this manner, the evidence in Bayesian updating (denominator in Equation C.1) becomes the network risk in Equation 3.5. This equivalence indicates that the consequence function $C[T(\boldsymbol{\theta})]$ needs to be non-negative, i.e., asset damage does not improve the transportation performance. This is valid for most performance indicators including the flow-based indicator used

herein. However, if total travel time is used, there might be rare cases when damaging an asset may decrease total travel time as in the case of Braess paradox (Bell & Iida 1997). In practice, this is more of an issue related to network design rather than network risk assessment. Therefore, negative $C[T(\boldsymbol{\theta})]$ can be set to zero for network risk assessment based on total travel time.

APPENDIX D GENERATING REGIONAL HIGHWAY NETWORK MODELS

Transportation assets in an asset management system are typically organized in a relational database and presented as tables of bridge information. Although GIS data of individual assets may exist in this database, these data are not directly available as network models suitable for system-level performance analysis. Therefore, an automated procedure is developed to establish a graph model for a particular region of interest.

Geospatial data of transportation structures and road networks are extracted from OpenStreetMap[1], an open collaborative geographic database (Contributors 2022), through its application programming interface (API). Highway networks can be recovered by focusing on road segments labeled in OpenStreetMap[20] as "motorway", "trunk", and "primary" (Contributors 2022). It should be noted that the geographic data obtained from OpenStreetMap[20] are not the graph model needed for network analysis. In a geospatial database such as OpenStreetMap[20], road segments are represented as polylines, which are designed to depict the geographic paths of roadways. The term "nodes" in OpenStreetMap[20] refers to the points that make up a polyline. However, these nodes also include points that determine the shape of a curved roadway, not just significant points like intersections or endpoints of roads. Therefore, they do not always represent meaningful elements of a transportation network. Figure D.1 illustrates the process of converting polylines to proper links in a graph-theoretic network.

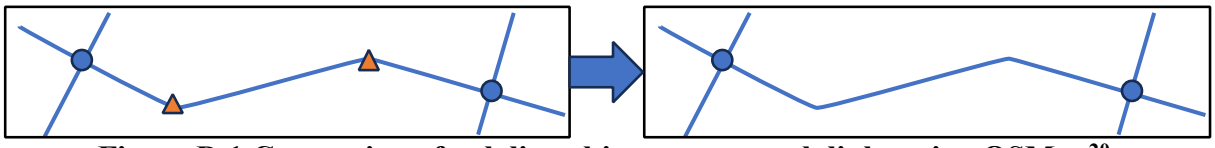

Figure D.1 Conversion of polyline objects to network links using OSMnx[20]

To achieve the conversion, OSMnx[20] (Boeing 2017) is utilized to extract and model roadway networks from OpenStreetMap[20]. The tool directly generates a directed multigraph for the street network in a specific region of interest. It can also convert the multigraph to a simple graph by preserving only the link with the shortest length among each node pairs. The generated networks are graph objects in NetworkX[20], a Python package for complex networks (Hagberg et al. 2008).

[1] The U.S. Government does not endorse products or manufacturers. They are included for informational purposes only and are not intended to reflect a preference, approval, or endorsement of any one product or entity.